Università degli Studi di Catania

International Ph.D. in Chemical Sciences
XXV Cycle

Davide Sapuppo

Chemical effects in cluster SIMS depth profiling of polymer-based materials

Advisor: Prof. A. Licciardello
Coordinator: Prof. G. Musumarra

Ph.D. Thesis

A.A. 2011-2012

Università degli Studi di Catania

Dottorato di Ricerca Internazionale in Scienze Chimiche
XXV ciclo

Davide Sapuppo

Effetti chimici nel *cluster SIMS depth profiling* di materiali a base polimerica

Tutor: Prof. A. Licciardello
Coordinatore: Prof. G. Musumarra

Tesi di Dottorato di Ricerca

A.A. 2011-2012

TABLE OF CONTENTS

1. Introduction

Studies on surfaces and thin films play an important role in materials science, since surface and thin film properties are pervasive in many technological areas. In many applications, as well as in fundamental studies, it is very important to obtain detailed and spatially resolved chemical information, both laterally (chemical imaging) and in-depth (depth profiling) in order to get, ideally, a 3D compositional picture of the material. Such statement, valid for any kind of material, is very important for molecular materials, such as polymer-based systems. Indeed, in spite of the increasing technological demand of detailed and spatially resolved molecular information from such materials, in fields ranging, just as an example, from organic/polymer devices (OLEDs, displays, organic or plastic solar cells etc.), to barrier films for food packaging, to automotive or aerospace coatings, there is a lack of techniques capable to provide such information. In particular, no "universal" technique is presently available that is able to discriminate among different organic layers, although in many of the above mentioned applications "multilayered" organic (or, more specifically, polymer) thin films are involved.

Since several years, a primary role in the study of surfaces and thin films is played by secondary ion mass spectrometry (SIMS), that is based on the emission ("sputtering") of atoms and molecules from a surface under irradiation with an ion beam ("primary ions"), and on the mass spectrometric analysis of the charged fraction ("secondary ions") of the emitted material. The technique can be used for obtaining detailed chemical information from the outermost surface layers as well as in-depth compositional information. In particular, an instrumental arrangement using a time-of-flight mass analyzer (ToF-SIMS), is especially well suited for providing information on the uppermost surface layer(s) of solids, in the

operational mode known as “static SIMS”[1]. State-of-art ToF-SIMS provides high resolution ($M/\Delta M$ >10000) surface mass spectra and chemical maps with a lateral resolution better than 50 nm. As to in-depth analysis, it can be achieved with various experimental arrangements, all involving the sputter removal of surface layers (“dynamic SIMS”). Depth profiling can be accomplished either in continuous mode, as in quadrupole- or magnetic sector-based instruments, or in an alternate way (“dual beam mode”), as in time-of flight instruments. Whatever the experimental arrangement adopted, sputter-erosion-based depth profiling involves rearrangements and modifications inside the material under analysis, due to processes caused by its interaction with the primary ion-beam[2]. Generally speaking, these processes “destroy” part of the chemical information that can be instead obtained in “static” conditions (that however confine the study to the very surface of the sample) so that the in-depth information is usually limited to the elemental distribution only, and often with possible artifacts[3]. In the case of “hard” materials, for example, the measured depth profile is influenced by effects such as radiation enhanced diffusion, ion-beam mixing, gibbsian segregation, and by the ion beam-induced morphological modifications of sample surface. In the case of “soft” matter (such as molecular solids, natural or synthetic polymers, biological specimens), there are further and more spectacular effects due to ion beam-induced chemical reactions. For these materials, the modifications generated by the ion-material interaction, are often so drastic to clear the “memory” of original material[4].

The above described situation has changed in the last decade, with the introduction in SIMS of polyatomic ion beams (SF_5^+, metallic clusters, fullerene ions are the most common), in place of the “traditional” mono- or bi-atomic

projectiles (such as Ar^+, O_2^+, Ga^+, Cs^+). The use of polyatomic (or "cluster") projectiles grew so much in importance that it is nowadays considered a particular field of the SIMS technique, the so-called "**cluster SIMS**"[5]. In fact, because of the particular characteristics of the interaction between the polyatomic ion beam and the surface (including low penetration depth, high density of deposited energy, non-linear effects caused by the time overlap of collision cascades) peculiar effects are observed. In particular, the use of cluster projectiles produces a strong increase of the ionisation probability of the sputtered particles, and this affects positively the sensitivity of the technique, as well as (due to the increase of the signal-to-noise ratio) its lateral resolution that, for molecular materials, typically increases by an order of magnitude (from ~1000 to ~50 nm)[6]. Furthermore, in many materials, both organic and inorganic, an increase of sputtering yield is observed that, again, helps in extending the analytical capabilities of the technique.

In addition to the above described advantages of cluster SIMS, a new exciting – and in some extent unexpected - feature of cluster SIMS is its capability to provide – although under certain conditions and with some limitations - molecular information along the depth of organic and polymer materials, i.e. to provide "molecular depth profiles". Due to its relevant fundamental and applicative implications there is nowadays a large growth of studies on cluster-SIMS, both on the experimental and the theoretical aspects, most of the latter not yet completely elucidated.

From the experimental point of view, cluster SIMS opened many perspectives both in imaging and depth profiling of organic-based systems, providing for the first time a methodology able – at least in principle - to produce 3-D chemical

maps of molecular materials. In the case of "classic" depth profiling, obtained by mono- or bi-atomic ion beams, due to the above mentioned damaging effects of the beam, it is impossible to obtain a molecular depth profile from an organic material, since the intensity of structure-related secondary ions (often referred as "molecular signals") collapses to zero as soon as the "static" limit is exceeded (i.e. after the sputter removal of a few percent of a "monolayer"). By contrast by using polyatomic primary ions, molecular signals are often observed from many organic materials well beyond the "static" limit, thus allowing us to obtain molecular depth profiles of organic (polymer) materials. The most typical polyatomic ions used for this purpose are SF_5^+, C_{60} and, very recently, massive Ar_n clusters ($700<n<3000$)[7, 8, 9, 10, 11].

The most common explanation for the preservation of molecular signals beyond the static limit under cluster bombardment is related with the low penetration depth (that tends to become comparable with the sampling depth) and with the high energy density deposited in the impact region. This is thought to make the polyatomic particle able to sputter away, more or less quantitatively, the volume of material damaged by the ion-solid interaction. Such a picture is supported by computational (molecular dynamics-based) simulations[12, 13], that evidence how a single impact of the polyatomic ion – at variance of the monoatomic one - removes a large fraction of the impact-damaged area, thus avoiding the build-up of chemical damage that is responsible of the failure of depth profiling for molecular materials. A comparison of the effects of monoatomic and cluster projectiles on a solid surface is depicted in figure 1, obtained from MD simulations[14, 15]. However, this important effect, alone, does not explain completely the experimental results, as the erosion behaviour of

molecular materials, is largely influenced by the chemical behaviour of the analyzed system and by the type of ion beam utilized[16, 17, 18].

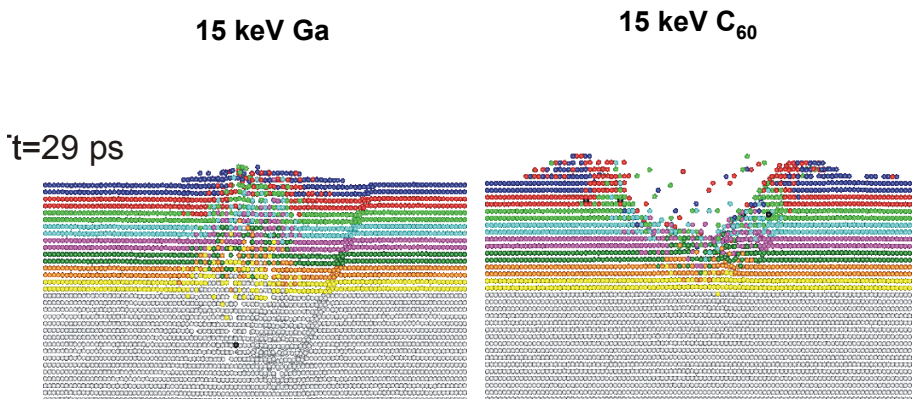

Fig. 1 - MD simulation comparing the impact of a monoatomic and of a cluster ion on a silver surface.

From http://galilei.chem.psu.edu/sputtering-animations.html

In fact, while some polymers like polyacrylates, and some molecular solids like Irganox 1010 or trehalose, are easily "profiled" with SF_5^+ or C_{60}^+ [19, 20, 21, 22], other materials like polycarbonate or polystyrene, polyethylene, PET, are not "profiled" in these conditions. Moreover, it turns out that the erosion behaviour of some of these materials is influenced by temperature and by the presence of reactive gases in the residual atmosphere of the UHV chamber of the SIMS spectrometer, again pointing towards a role of chemistry in the mechanisms involved in cluster beam sputter erosion of soft matter and of polymers in particular.

Aim of this PhD experimental work is that of giving a contribution in the elucidation of the chemical effects involved in cluster SIMS molecular depth profiling of polymers and in the development of methods capable of extending the applicability of such a technique to systems that are difficult to investigate due the "adverse" chemical reactions triggered by the interaction with the ion beam. In particular the effect of a reactive gas, namely nitric oxide, in C_{60} SIMS depth profiling of polymer based systems has been investigated, starting with some model systems and then extending the study to more complex ones, such as multilayered samples or phase separated blends.

After an initial overview (chapter 2) of some the experimental and fundamental aspect of cluster beam interaction, relevant for cluster-SIMS depth profiling of polymers, the experimental results will be discussed in the next chapters. For the sake of better readability, a substantial part of the information regarding the experimental details will be given in the appendix chapter on materials and methods.

2. Cluster SIMS and molecular depth profiling

In the last two decades, with a strong acceleration in the last few years, many developments took place in the field of cluster SIMS, and several papers appeared in the literature about the influence of the experimental parameters (such as energy and type of cluster, angle of incidence, etc.) on ion yields, sputtering yields, amount of fragmentation observed in the spectra, in a variety of samples, including a large spectrum of molecular materials.

Parallel to instrumental developments and to the accumulation of experimental data, many efforts have been dedicated to the elucidation of the phenomena underlying the sputtering process induced by cluster primary beams that cannot be fully understood in the framework of the classical models based on the binary collision approach.

As far as cluster SIMS molecular depth profiling is concerned, many papers SIMS were aimed to explore the "profilability" of many molecular materials. Several studies, in particular, were dedicated to the SIMS molecular depth profiling of polymers, and many of them are reviewed in a paper of Christine M. Mahoney[5]. It is probably worth to discuss briefly the concept of "molecular" depth profile: for organic samples and soft matter in general (organic molecules, molecular solids, polymers) a depth profile is called "molecular" when a signal that is related to the structure ("molecular" signal) is retained along the whole investigated sample thickness. From the variety of experimental results available, the question arises about when a molecular depth profile can be considered successful. Usually a depth profile of an organic layer is considered completely successful when a steady state intensity of the considered signal is reached and it remains constant until the interface with the underlying layer, if any, is reached. Also, satisfactory sharpness of the interface, i.e. a good depth resolution, is

usually required. Typical successful depth profiles are reported for example in the case of C_{60}-SIMS of PMMA films on silicon[9]. By contrast, molecular depth profiling is completely unsuccessful when no retention of any molecular signal is observed beyond the static limit, i.e. beyond the ion fluence threshold after which the overlap of ion tracks cannot be neglected[2]. This is for example the case of high molecular weight polystyrene profiled with C_{60}^+ or SF_5^+ ion beams[9, 23]. The above depicted cases are the extreme ends of a graded variety of situations that could be defined "quasi-successful" depth profiles. These situations occur when the molecular signal is only partially retained and/or not maintained constant along the depth. These different cases are described more quantitatively by Cheng, Wucher et al[24, 25, 26] in terms of efficiency of removal of the damage produced by the beam (clean-up efficiency). The Wucher's model, however, does not imply any particular mechanism for sputtering and for damage creation. Other papers, *vice versa*, pointed towards the elucidation of the peculiarities of the cluster-beam interaction with solid surfaces (either organic or inorganic) and on the understanding of the chemical events, triggered by the beam-solid interaction, that contribute to the sputtering behaviour of organics and polymers. In the following some of the basic physical aspects of the cluster solid interaction, mostly studied by means of molecular dynamic simulations, and the role of chemistry in the molecular depth profiling, will be discussed, with particular attention to molecular depth profiling of polymers.

In the most recent years, the search for an "universal" way of molecular depth profiling has been an open challenge: in fact, although the introduction of cluster ion beams represented a breakthrough for the possibility of molecular depth

profiling of polymers (e.g. with the introduction of C_{60} ion sources), it turned out that, as mentioned above, some polymers are amenable of molecular depth profiling while others aren't. The two different behaviours can be explained (at least in the case of polymers) in terms of prevailing cross-linking or chain scission reactions. According to a terminology coming from radiochemical studies involving UV, γ-ray, neutron or electron irradiation[27] polymers are classified in two classes, type I and type II respectively. In type I polymers cross-linking is the prevailing radiation-induced mechanism, while type II polymers mainly undergo to chain scission reactions, often with loss of monomers ("unzipping" depolymerization). Not surprisingly, only type II polymers are easily profiled by means of "cluster SIMS", as they produce volatile molecules that are pumped down in the UHV chamber of the SIMS instrument, and this helps in the cleaning-up of the damage, an important requisite for molecular depth profiling. Type I polymers include polyethylene, many polyolefins and, as in case of polystyrene and bisphenol-A-polycarbonate, they are often characterized by the presence of aromatic rings in the structure. Type II polymers include polymethylmethacrylate and others[28].

On the basis of the above considerations, Mahoney[5] extends the same classification to depth profiling of polymers. Indeed she reports a list of polymers, that are divided in two categories, type "I" and "II", on the basis of the profilability (difficult in the case of prevailing crosslinking process, easier in the case of the chain scission).

In this Ph.D. thesis a similar notation will be adopted, but the "type" will refer to the observed behaviour than to the polymer itself. Indeed there are several examples of polymers which radiation induced behaviour (type I or II) depends on

the particular conditions adopted, such as temperature or type of cluster beam used.

An illustrative example of temperature-dependent behaviour is given by the case of poly-α-methyl styrene (PAMS) that, under C_{60} ion irradiation, "switches" from "non profilability" to "profilability". As shown in fig. 2, this polymer exhibits a type I behaviour at room temperature (and up to 110°C), that is gradually changed in a type II behaviour from 110°C to 160°C[9]. Temperature effects are also observed in PMMA under C_{60}^{+} or SF_5^{+} bombardment[9, 23]. Such a temperature dependence recalls the behaviour of PMMA under high energy (~10^2 keV) monoatomic ion beam irradiation, in conditions that are quite different from

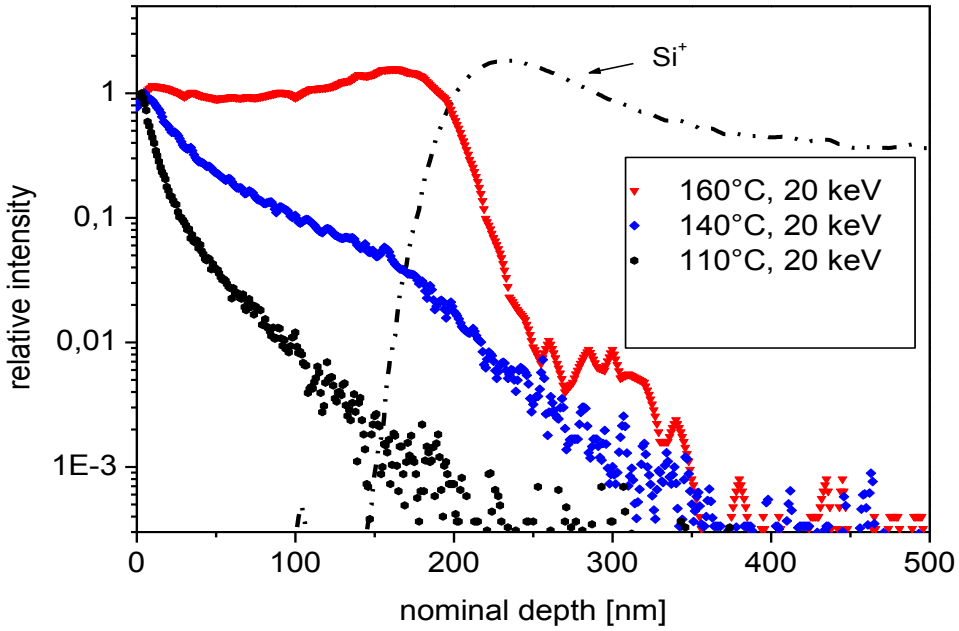

Fig. 2 - Effect of temperature on PAMS depth profiling (from ref. 9)

those suitable for SIMS. Indeed, PMMA undergoes ion beam-induced depolymerisation above a certain temperature threshold. Considering that a pure thermal depolymerization process occurs at T > 360 °C, the observed phenomenology can be explained by hypothesizing that part of the energy required to overcome the potential energy barrier for depolymerization can be supplied by the ion beam[29, 30]. In the case of "monoatomic" SIMS (with primary energies of the order of few keV) PMMA mostly undergoes side-chain scission and cross-linking[31], with an overall type I behaviour similar to that of polyolefins, unless temperature is increased to about 170°C[9].

All above clearly suggests that the different behaviour of polymers (either different macromolecules or the same one at different temperature) with respect to molecular depth profiling is connected with different (and competing) reaction pathways followed by the active species (often radicals) produced by the ion-matter interaction. In this framework, the production of volatile low molecular weight fragments favours the ablation of damage and the observation of a "molecular depth profile".

The behaviour of organic samples, and polymers in particular, under ion beam irradiation (usually monoatomic high energy ions) has been studied since several decades. Many studies were performed at very low ion doses in order to study the "primary" chemical events triggered by the beam-solid interaction. Often these studies retain concepts extensively used in the classical radiochemical studies involving the use of energetic photons (from UV to gamma-rays), electrons, neutrons. Among these concepts is the G-value, i.e. the number of events produced by 100 eV of absorbed energy or the previously cited

classification in “type I” and “type II” categories. The parallelism between classical radiochemistry and the ion beam bombardment is based on the assumption that in both cases similar species are formed in the polymer as direct consequence of the interaction with the energetic particle (with consequent energy transfer from the particle to the material), and that the subsequent evolution of the system involves similar complex mechanisms, often involving free radical intermediates.

In spite of the similarities with other energetic particles, however, the ion-matter interaction is characterised by some peculiarities. In particular a substantial amount of energy, especially in the experimental conditions of SIMS experiment, is transferred to the target via momentum transfer processes, within the volume of the so-called collision cascade. These collisional processes play an important role in the sputtering process on which the SIMS experiment is based. Indeed, in the framework of the LSS theory[32] and its subsequent refinements, we classically refer to the sputtering process as a phenomenon strongly related to the collision cascade induced by the primary ion beam[33], in which the contribution of the electron stopping power is negligible with respect to the nuclear stopping power[34]. It must be stressed that, due to the very short mean free path of atomic species in a solid material, the species sputtered away from the material originate from the uppermost layers of surface, although the penetration depth of the primary ions (that in turn depends on its mass and energy) is usually much deeper, so that, as in the case of keV monoatomic primary beams, the depth damaged by the ion irradiation (altered layer) is much thicker than the analysed depth. This fact, while affects the depth resolution in inorganic samples, makes it difficult or impossible the molecular depth profiling of organic samples. In the case of polyatomic

beams, due to their lower penetration depth with respect to monoatomic ions of the same energy, the thickness of the "altered layer" can become comparable with the sampling depth. Actually it is nowadays recognized that the success of cluster SIMS in molecular depth profiling is due to this similarity of sampled and damaged depth joined with the large increase of the sputter yield of the material. The combination of these two factors can produce, ideally, the simultaneous erosion/removal (during a single ion impact) of the (damaged) volume involved in the interaction.

It must be remarked that the high sputtering yields observed in polyatomic ion bombardment, as well as the relatively large ionization yields, are non-linear ones. In other words, the effect produced by a generic cluster A_n with energy E, is not simply n times the effect of a monoatomic ion A with energy E/n. These non-linear effects are mostly connected with the large density of energy (and in its space distribution) deposited by an impact. In the case of polyatomic ions this results in a strongly energized and surface-localized impact region. In this case, the LSS theory, and the related concepts of projected range and collision cascade, are no more applicable to the emission process caused by the cluster ion impact phenomenon that, under many aspects, is more similar to an "ablation" process (like those caused by laser beam irradiation), rather than a classic "sputtering" one, even if in literature the majority of authors still refer at the cluster SIMS induced erosion as a strongly enhanced sputtering process. Presently, a great contribution to the understanding of the erosion process under cluster beam irradiation derives from MD simulations, and studies aiming to generally clarify the cluster SIMS bombardment of various target samples are continuously in

progress into the SIMS community, as reviewed by B. J. Garrison and Z. Postawa[35].

The relationship and similarities between cluster ion beam impact and ultrafast laser irradiation was investigated by Urbassek et al[36, 37] by molecular dynamics simulations, in which authors refer at the interested volume of sputtering and ablation as a highly "energized volume". In this simulation, a self-impact between 500 keV Ar_{100} cluster ion beam and an Ar amorphous solid is considered, resulting in a particular sputtering process, named "phase explosion", that occurs *via* gasification of the high energized (and surface-localized) zone. These processes occur out of the equilibrium, in contrast with the thermally induced evaporation.

The parallelism between laser ablation and cluster beam sputtering can be useful for interpreting the behaviour of PMMA. Indeed by comparing ultrafast UV laser irradiation with cluster ion impact of PMMA, some similarities are found in the erosion process, that, according to the models, occur only beyond a threshold value of excitation (energy deposited in target) for both the phenomena. This comparison can be extended to the chemical processes induced by the irradiation. In this respect useful indications are provided by the simulations of the UV ablation of PMMA[38], involving the radical Norrish reactions type IA-IB (side chain cleavage) and type II (main chain cleavage), that are considered responsible of the easy depolymerization of PMMA and of polyacrylates under high energy density conditions. An interesting summary of the MD simulations about the sputtering *via* nanocluster beams has been recently provided by Delcorte et al[39], in which the various parameters involved in cluster SIMS molecular depth profiling are considered. In particular, the following aspects are taken into account: type of

cluster beam, energy, range, crater shape, mass, molecular desorption, incidence angle, ion beam induced chemistry, providing an interpretation based on the assumption that the impact of C_{60} produces a lot of (reactive) carbon radicals, resulting in a large number of induced crosslinks, with respect to the inert argon, that produces a lower amount of damage. As can be easily forecast, the ideal beam for "universal" molecular depth profiling has to satisfy some important requirements, and one of the most important is certainly that of the minimum of damage accumulation into the material.

Rading et al[40] reported a study about the differences in depth profiling of type I polymers with Ar massive clusters and fullerene clusters, by comparing the amount of the "information depth" (located above) and the amount of the "damage depth" (located below), also in dependence on the incidence angle used. When the information depth is less than the damage depth, a loss of molecular information is observed, as in the case of PS and PC with 45° incidence angle. *Vice versa*, when the damage depth is less than the information depth, as in the case of PS and PC with grazing incidence angle (70° with respect to the normal to the surface plane), they observe an increase of the yield of secondary ions, although a certain damage cannot be neglected. The ideal experimental condition is to obtain zero damage depth and in this way full molecular information should be successfully retained. In the case of PC and PS this condition can be provided by the massive Ar clusters GCIBs), while in the case of PMMA and other polyacrylates the use of C_{60} is sufficient.

Such experimental findings are confirmed by calculations. MD simulations[41] comparing the bombardment with various cluster beams, including massive Ar clusters, show how the GCIB Ar_n^+ impact occurs closer to the surface than the C_{60}

impact, resulting in a more efficient erosion via "ablation" of the minimal damage induced. The represented scenario can be interpreted in terms of:

- radius of the originated crater (that originated by GCIBs is higher than that produced by C_{60})
- penetration depth (lower for GCIBs than for C_{60})
- amount of damage (reduced in the case of GCIBs), with easier removal by the large cluster beams.

In other words, if the C_{60} impact could be assumed as a hemispherical crater, the Ar_n^+ crater could be considered as a "dip" in the surface, which results in a negligible induced damage with respect to C_{60}. This effect of minimization of the damage accumulation makes successful molecular depth profiling with GCIBs also in the case of polymers which are known to suffer ion beam induced crosslinking damage with C_{60}, like polystyrene and polycarbonate[42] .

In view of all above, probably the best choice of projectile for molecular depth profiling are the giant gas argon clusters. However, a possible alternative approach for limiting the ion-beam induced damage during depth profiling of polymers is that of understanding the basic mechanisms underlying the damage processes and trying to minimise them.

There are different reasons for attempting different approaches. Among others, i) the fact that GCIBs suffer some limitations in profiling inorganic systems so they are difficult to apply also in hybrid organic/inorganic systems; ii) the possibility to extend, without expensive upgrades, the applicability of the widely disseminated instrumentation with fullerene ion sources and, last but not least, the gain of fundamental knowledge arising from the development of these alternative approaches.

The chemical modifications induced by ion-beam irradiation in polystyrene were largely studied in the past, with several contributions by Licciardello et al[43], Calcagno et al.[44, 45, 46], Klaumünzer et al[47], aimed to the elucidation of the crosslinking reactions undergone by polystyrene. Although some questions about ion beam induced chemistry of PS remained unsolved, it became apparent that a major role was played by the density of energy deposited by the beam[46].

Recently, some MD simulations have been performed for emulating the highly aromatic polystyrene. One of these simulations[48], reported a study on the chemical damage resulting from cluster bombardment of solid benzene, although no reference is made to the crosslinking phenomenon. There is actually some lack of simulation data on crosslinking effects under ion bombardment, probably connected with the difficulties in mimicking the formation of new bonds in the framework of MD calculations.

Brenes et al.[49] compared experimental end theoretical results of 20 keV C_{60} cluster bombardment onto molecular solids like benzo[a]pyrene (experimentally obtained as evaporated film onto a substrate) and crystalline benzene (calculated by coarse-grained MD simulation), being the latter the "building block" of benzo[a]pyrene and other PAH. Further, a comparison with Ni{0 0 1} was performed, in order to evidence the differences between a molecular and an atomic (metallic) system. This comparison resulted in a different sputtering process of the molecular system with respect to the atomic one. Also, the impact of C_{60} with the molecular surface provides a very energized and surface localized volume, resulting in a fully desorbed region, composed primarily by molecular fragments of the target, in off-normal directions, at variance of the behaviour of Ni atoms, fully desorbed in a normal direction.

Again, the calculations do not simulate the formation of new bonds. Probably for this reasons they do not explain the behaviour of some polymers, like PS or PC, that undergo crosslinking and extensive damage under C_{60} irradiation. On the other hand existing experimental data indicate that it is possible to interfere with ion-beam triggered reactions, so that there is some room for the search of strategies able to influence the damaging effects of the beam by blocking, or at least limiting, the adverse ion beam induced reactions and possibly favouring the advantageous ones (like those leading to fast production of volatile species).

The importance of chemical factors, and the possibility of influencing the ion beam induced reactions that lead to damage, was demonstrated by the previously cited paper by Moellers et al., who obtained C_{60} molecular depth profiles of poly-alpha-methylstyrene by simply increasing the temperature of about 50 degrees and even a molecular depth profile of PMMA under Ga irradiation again by increasing temperature[9], and by Houssiau and co-workers[50, 51], that proposed the use of caesium at ultra low energy and successfully profiling polycarbonate.

Very recently, the use of water vapour, directly supplied closely to the impact region[52, 53] , was proposed as another way to interfere with the beam induced chemistry, also with the aim of increasing the production of ions by protonation.

Finally, the use of Nitric Oxide-assisted C_{60}, was proposed by our research group[54, 55, 56, 57], and on this strategy focuses this PhD thesis. As it will be shown in the next sections, this strategy allows us to extend the applicability of C_{60} SIMS to a larger variety of polymer-based systems, including type II behaving polymers and hybrid organic/inorganic systems, the latter quite difficult to profile with GCIBs.

3. Experimental Results

3.1 Outline.

In this chapter the experimental results obtained during this Ph.D. work will be presented and discussed. In the first part (3.2) a comparison between the "classic" monoatomic SIMS and the novel cluster SIMS, with focus onto model polymer materials, is reported. Also, the effect of nitric oxide on depth profiling in both cases is discussed, and the influence of partial pressure of nitric oxide will be examined also in relation with the basic chemical processes involved.

The following section (3.3) is dedicated to the application of the NO-assisted C_{60}-SIMS to multilayered polymer systems, including hybrid polymer/metal layers.

Finally, the application is extended other more complex materials (3.4) like random copolymers, immiscible polymer blends and polymer/additive systems, in order to "test" the potentialities of this technique on a variety of materials of technological and applicative interest.

3.2 Ar and C_{60} SIMS depth profiling of model polymers.

It is useful to begin the presentation of the experimental results with the data on dual beam SIMS depth profiling of simple model polymer samples, obtained by using either monoatomic (Ar^+) or polyatomic (C_{60}^+) ions as sputter beam and Bi_3^+ as analysis beam. Experiments were performed either in the "standard" operational conditions (i.e. in UHV without the presence of reactive gases during analysis) or in the presence of a partial pressure (1.5×10^{-5} mbar) of nitric oxide. The polymers chosen are polystyrene (PS), poly-α-methylstyrene (PAMS), polymethylmethacrylate (PMMA) and polyacrylic acid (PAA). Data will be presented and discussed by starting from the measurements in the absence of NO and then in the presence of NO:

3.2.1 Profiles in the absence of NO

First of all, let's discuss the results on polystyrene. For this type I polymer, molecular depth profiling has been already demonstrated to be unsuccessful not only by using "classical" monoatomic Ar primary ions, but even by using C_{60}[9]. The damage accumulation that, according with previous studies with higher energy beams on this kind of polymer[58, 59, 60], is thought to be due mostly to ion beam-induced crosslinking reactions, is so extensive that no retention, along the depth, of any molecular signal is observed. In figure 3 the profile obtained by sputtering with a fullerene beam is presented. The intensity of structure-related signals drops to the noise level as soon as the static limit is exceeded. Similar results, not reported here, are obtained by using Ar primary ions.

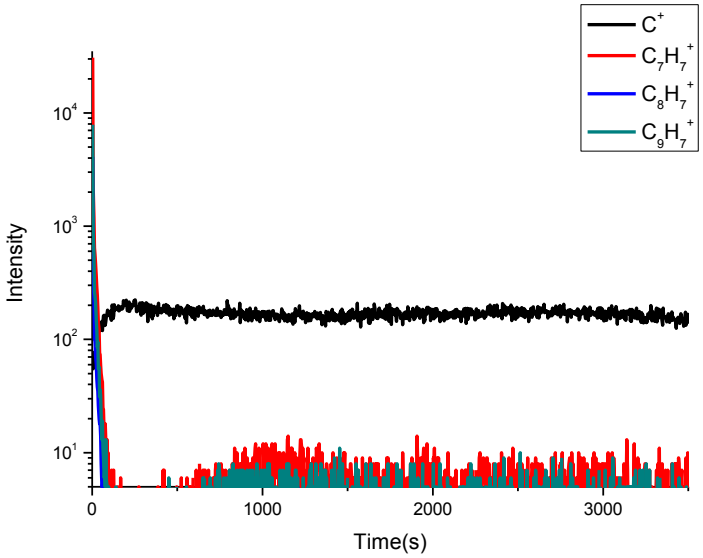

Fig. 3 – C_{60} depth profile of PS in absence of NO.

Another model polymer with type I behaviour under Ar and C_{60} irradiation is PAMS. This polymer is an interesting one, since it displays peculiar temperature behaviour: as already mentioned, under C_{60} irradiation it is known to switch to type II at sufficiently high temperature[9] . From the structural point of view PAMS is very similar to polystyrene but, due to the presence of a methyl group on the benzylic carbon, it has a quaternary carbon in the main chain, and this in some respect makes it similar to PMMA. Anyway, at room temperature and in the absence of nitric oxide, PAMS displays a behaviour virtually superimposable to that of PS. For this reason, in this section we report just the C_{60}-SIMS depth

profile (fig. 4) where the drop of molecular signals beyond the static limit is evident. .

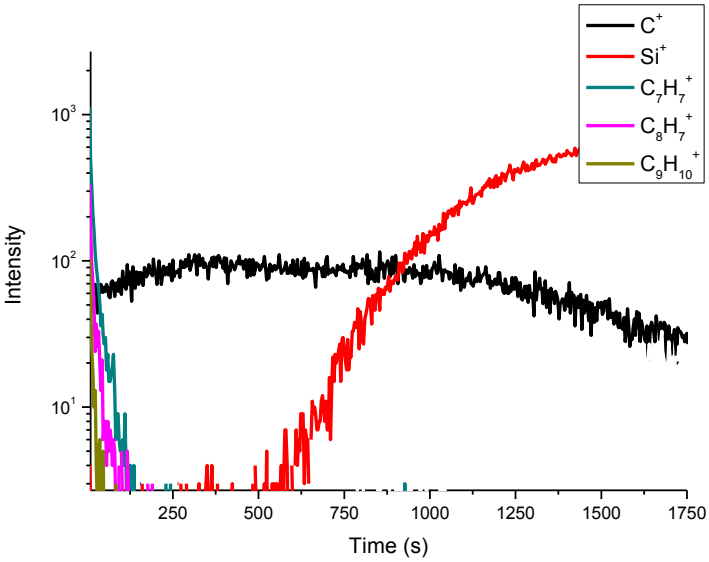

Fig. 4 – C_{60} depth profile of PAMS in absence of NO.

The model polymer of choice as paradigmatic of the type II behaviour under C_{60} irradiation is polymethylmethacrylate. In the following figures 5-6 the depth profiles of PMMA are reported, obtained by using, respectively, Ar or C_{60} primary sputter beams, and again Bi_3^+ as analysis beam in both cases.

As known from the literature[19], the use of polyatomic ions – at variance of monoatomic ones - allows to obtain a molecular depth profile of PMMA. Indeed the structure-related signals, namely the protonated repeating unit

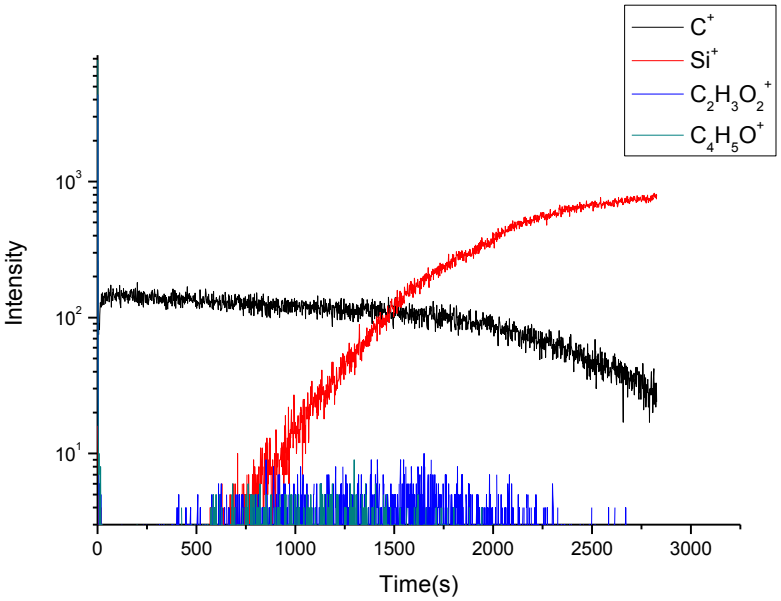

Fig.5 - Ar depth profile of PMMA in absence of NO.

(m/z 101) and the characteristic fragment at m/z 69, are detected with constant intensity until the PMMA film is completely removed and the interface with the silicon substrate is reached. By contrast, under Ar bombardment only aspecific signals, such as C^+ and $C_xH_y^+$ are observed

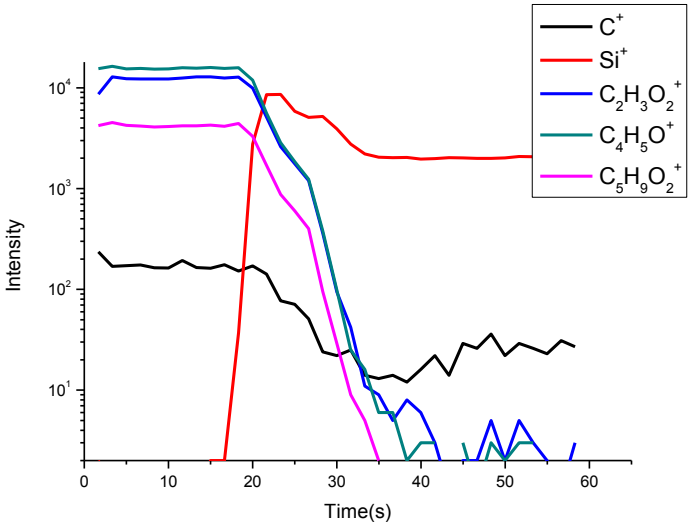

Fig. 6 - C_{60} depth profile of PMMA in absence of NO.

with appreciable intensity along the profile. It is also worth to note that the sputter rate with Ar ions is much lower than with fullerene, although comparable beam currents are used, as evidenced by the shorter time needed for reaching the interface with substrate (for the same film thickness). Finally, in figures 7 and 8 the depth profiles of polyacrylic acid (PAA) with Ar and C_{60} primary ions are reported.

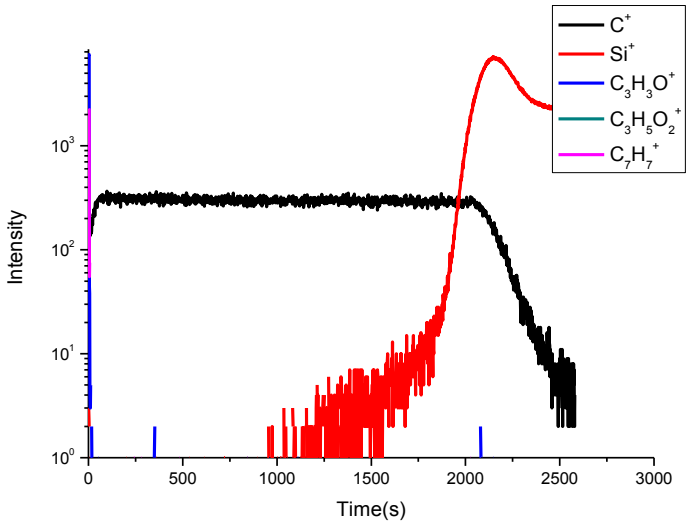

Fig. 7 - Ar depth profile of PAA in absence of NO.

Analogously to PMMA, a successful molecular depth profile is obtained for PAA when C_{60} ions are used instead of the "classical" Ar projectiles. Furthermore, an enhanced sputter rate is also observed with the fullerene beam.

The above results confirm that the use C_{60} is a good choice in order to obtain good molecular depth profiles in some classes of polymers, like polyacrylates, that under polyatomic ion irradiation (at variance of monoatomic ion bombardment) undergo ion beam-induced main chain cleavage and depolymerisation. By contrast, in the case of polymers like polystyrene and PAMS, no beneficial effect is produced by the use of a fullerene beam, because the cross-linking processes remain the major degradation pathways.

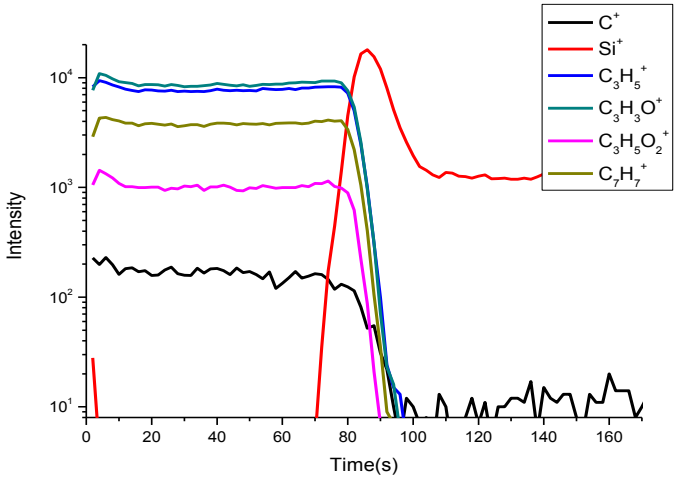

Fig. 8 - C_{60} depth profile of PAA in absence of NO.

.

3.2.2 Profiles with nitric oxide dosing

As discussed in the previous chapters, many ion-beam induced reactions in polymers involve radical intermediates. Depending on the particular chemical behaviour of each polymer, these radical reactions can produce chain scission (that ultimately results in the formation of low molecular weight volatile products) or the formation of new C-C bonds (cross-linking that, if repeatedly induced, leads to the formation of three-dimensional networks increasingly resembling a carbonaceous material). The idea underlying the use of nitric oxide dosing during

depth profiling of polymers is that this well known radical scavenger can interfere with, and possibly inhibit, at least partly, the ion beam induced radical reactions that produce the damage responsible for the failure of depth profiling of type I polymers.

In figure 9 we report the depth profile of a PS film on silicon, obtained with Ar ions in the presence of nitric oxide. The main observation is that, in spite of the introduction of NO in the analysis chamber, PS continues to exhibit a type I behaviour, i.e. no structure-related signal is retained beyond the static limit.

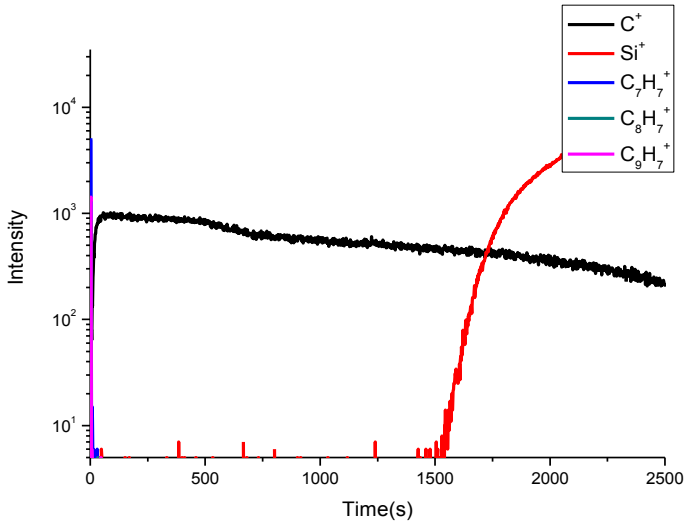

Fig. 9 - Ar depth profile of PS with NO 1.5x10^{-5} mbar.

Much more interesting results are found when nitric oxide (1.5 x 10^{-5} mbar) is used in conjunction with C_{60} bombardment. As it can be observed in figure 10, in this case structure related signals are detected along the whole thickness, although their intensity undergoes a strong reduction when the static limit is reached. After

the initial drop, however, the molecular signals remain constant until the interface is reached.

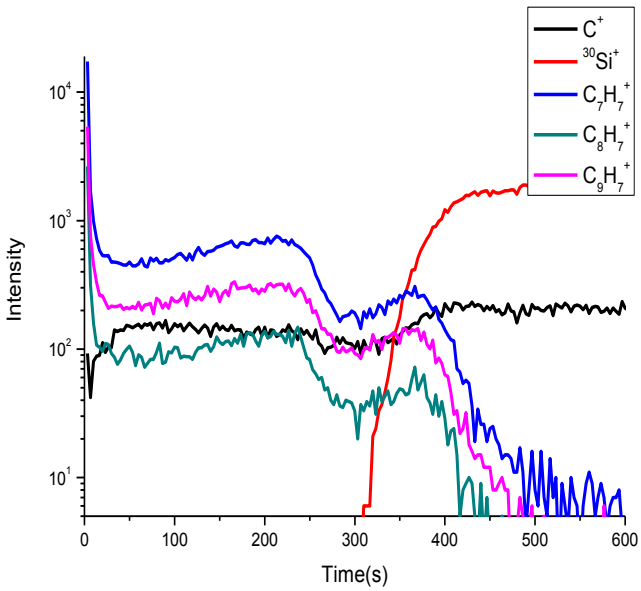

Fig. 10 - C_{60} depth profile of PS with NO 1.5 x 10^{-5} mbar.

In other words we can state that the presence of NO makes successful the C_{60}-SIMS molecular depth profile of polystyrene, that otherwise would be unsuccessful (see fig. 3). Additional interesting information comes from the comparison of the spectra reconstructed from the steady-state region of the profile and those obtained in static SIMS conditions from a fresh area of the same PS sample. As reported in figure 11, the spectra are very similar although some new peaks appear in the spectrum, due to NO-containing species. All above demonstrates that the presence of the radical scavenger is able to reduce the ion

beam-induced damage that is confirmed to be due, at least partly, to radical reactions.

The data above reported for PS prompt the interesting question why NO is effective in reducing the ion-beam damage when fullerene is used, while its effect appears to be negligible under Ar bombardment. A reasonable answer to such question can be given by reminding that the effect of NO is reasonably limited to the outermost layers of the polymer surface, since its

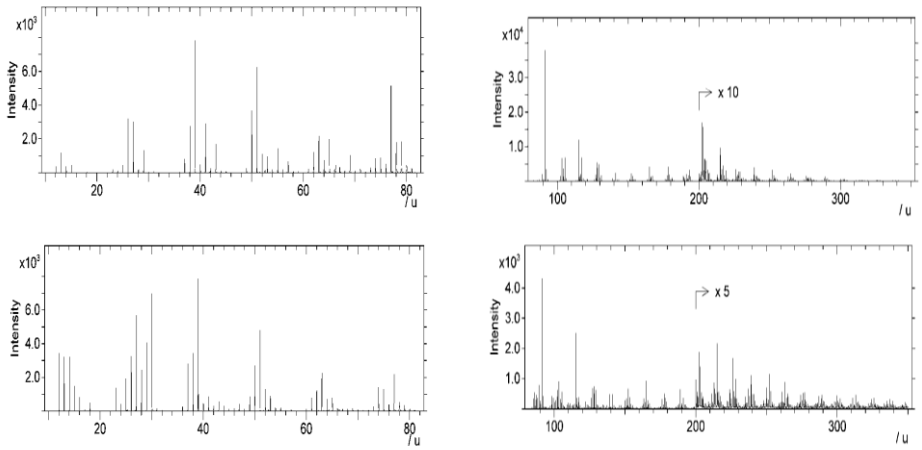

Fig. 11 - Comparison between static SIMS spectrum (upper part) and dynamic SIMS spectrum (bottom part), reconstructed from the steady state region of the profile of figure 10.

diffusion rate inside the polymer can be considered negligible compared with the sputter rate. On the other hand, as stressed in the previous chapters, the thickness of the layer interested in the interaction with the monoatomic projectile is much higher than that with the polyatomic one, so that more radicals can escape the inhibition effect of NO.

Results similar to those of polystyrene are obtained in the case of poly-α-methylstyrene. The C_{60}-SIMS depth profile, reported in figure 12 shows the retention of molecular signals, so that it can be considered a successful one. Furthermore, also for PAMS the reconstructed dynamic SIMS spectrum is

similar to that acquired under static conditions, again indicating a decrease of the damage accumulation due to the presence of NO (fig.13).

It is now interesting to evaluate the effect of nitric oxide (p_{NO} = 1.5 x 10^{-5} mbar) on the depth profiles of PMMA, obtained by using Ar or C_{60} ions (figures 14 and 15 respectively).

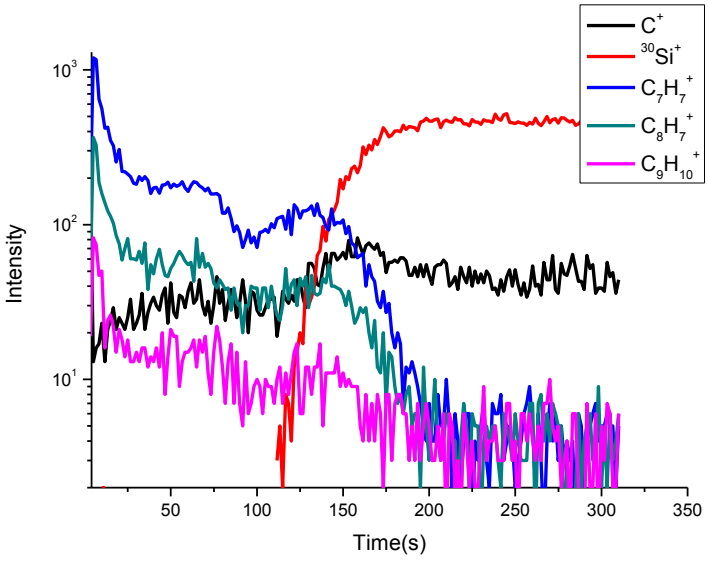

Fig. 12 - C_{60} depth profile of PAMS with NO 1.5 x 10^{-5} mbar.

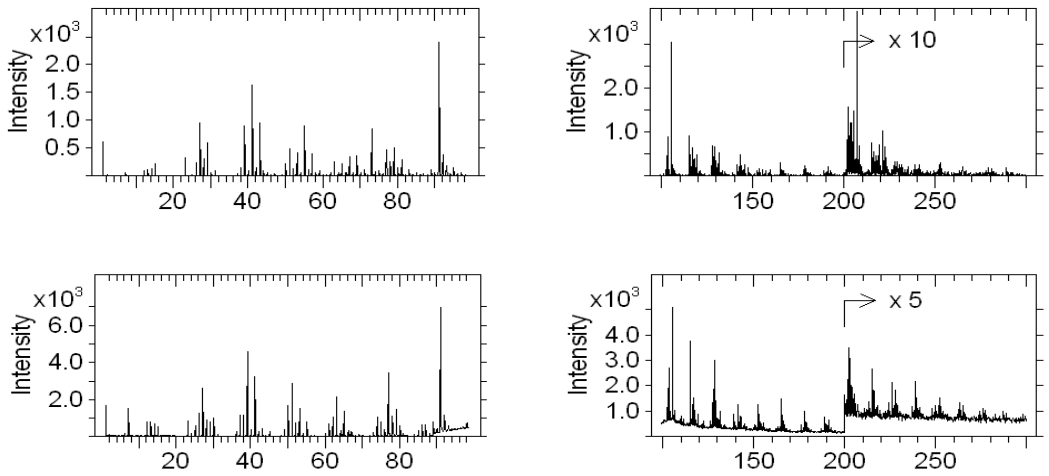

Fig. 13 - Comparison between static (up) and dynamic (down, reconstructed, with NO dosing) SIMS spectra of poly-α-methylstyrene.

The depth profile obtained with Ar and NO dosing (fig.14) surely cannot be considered a successful depth profile. However, at variance of the profile obtained in the absence of NO (see figure 5) some structure-related peaks are observed along the profile, although with a peculiar intensity trend. Moreover, from the comparison of the two profiles we note that the use of NO causes an increase of the sputter rate of approximately 3-4 times.

As to the profile of PMMA with C_{60}, obtained in the presence of NO (fig. 15), we observe that the effect of the radical scavenger is negligible, both on the

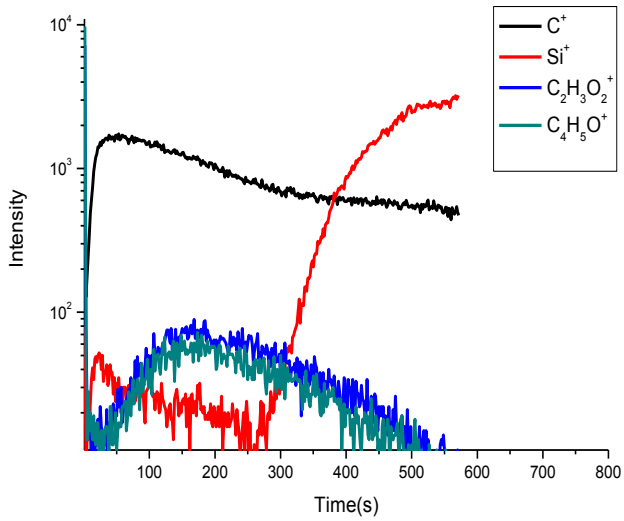

Fig. 14 - Ar depth profiling of PMMA with NO 1.5 x 10^{-5} mbar.

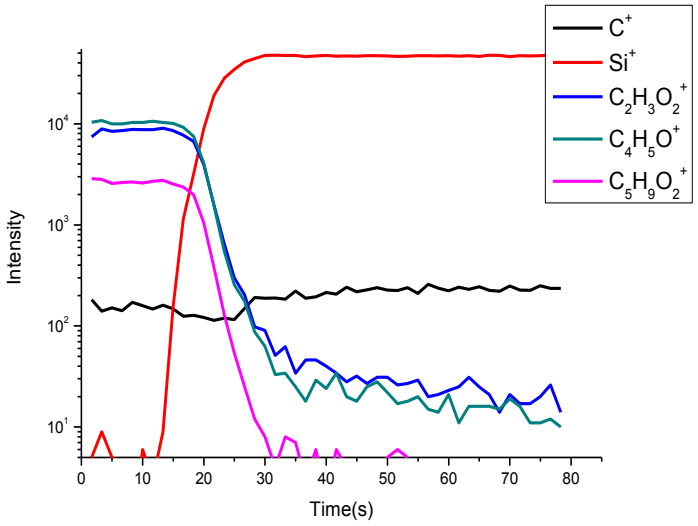

Fig. 15 – C_{60} depth profile of PMMA with NO 1.5 x 10^{-5} mbar.

intensity of the molecular signals and on the time needed for reaching the interface (compare with the profile of fig. 6 obtained without NO). The main difference between the profiles obtained with or without nitric oxide dosing is apparent at the interface and in the substrate region, were the silicon signal of the substrate is enhanced and its transient interface peak (due to the presence of native oxide on silicon) is suppressed in the presence of NO. Both effects are explained by the oxidizing effect of nitric oxide that acts on silicon in a similar way as oxygen, which in indeed widely used in depth profiling of inorganic thin films (either by oxygen dosing or as primary beam) in order to enhance the ion yield of silicon and to reduce matrix effects, such as the increase of positive ion yields from oxides compared to the elements).

Finally, in figures 16 and 17, the NO-assisted depth profiles of a polyacrylic acid film on silicon are reported. For this acrylic polymer, not unexpectedly, the results are similar to those obtained for PMMA. In particular, in the case of C_{60} depth profiling nitric oxide dosing produces significant effects only on the inorganic substrate signals. In the case of Ar depth profile (fig.16) the intensity of molecular signals along the profile when NO dosing is used is higher than in PMMA, although not constant as already observed for PMMA. Also, an enhancement of sputtering rate of 5-10 times is observed with respect to the profile obtained without NO-dosing.

Summarizing, the results shown above indicate that:

- in the case of polystyrene and PAMS, molecular depth profiling is achieved only by NO dosing in combination with the use of the fullerene primary ion beam;

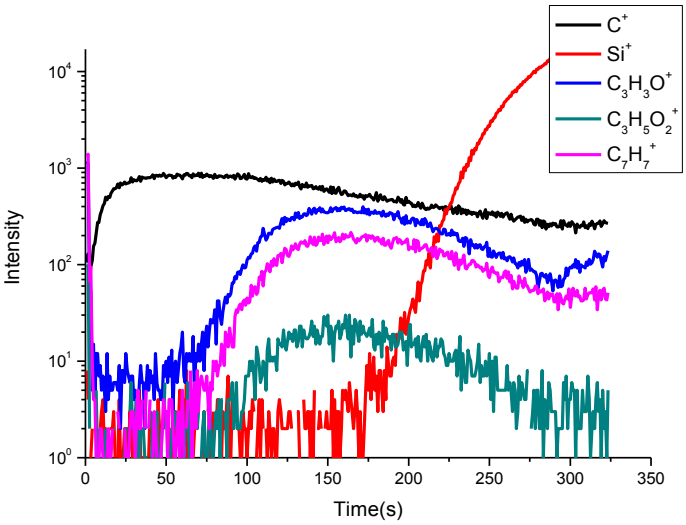

Fig. 16 - Ar depth profile of PAA with NO 1.5 x 10^{-5} mbar.

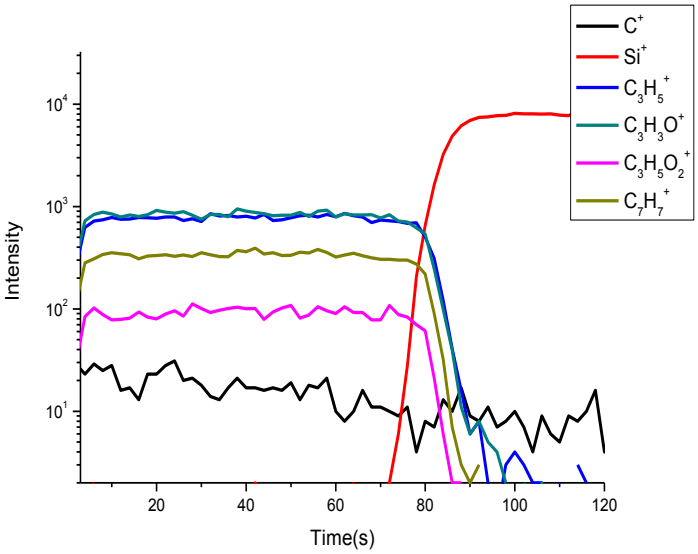

Fig. 17 - C_{60} depth profile of PAA with NO 1.5 x 10^{-5} mbar.

- in the case of PAA and PMMA, depth profiles obtained with Ar in the presence of nitric oxide display a partial retention of molecular signals, that is however not enough for considering such profiles as completely successful molecular depth profiles. When using a C_{60} beam on these polymers, good molecular depth profiles are obtained, irrespective of the presence of nitric oxide. A possible explanation of the lack of effects of nitric oxide on the sputter behaviour of the considered polyacrylates (in some respect an unexpected observation) will be given later, in the next section.

In conclusion, the above reported data indicate that nitric oxide dosing has a beneficial effect on C_{60}-SIMS molecular depth profiling of polymers when they display a type I behaviour, while the effect is virtually negligible (apart the interface regions with inorganics) when the polymer displays a type II behaviour. This indication candidates nitric oxide dosing as an interesting and simple method for widening the applicability of C_{60} depth profiling to "difficult" polymers such as polystyrene.

3.2.3 Effects of pressure of NO on depth profiles

In order to gain some further insight on the effect of nitric oxide in C_{60} depth profiling of polymers, and also with the aim of optimising the experimental conditions, experiments at different p_{NO} were performed. As mentioned in the previous part of this work, the experimental observations on cluster-SIMS molecular depth profiling of polymers show a quite strong correlation[5] between

the “profilability” of a polymer and its radiochemical (type I or II) behaviour[27] , i.e. the prevalence of main chain scissions or crosslinking under irradiation. In particular it is quite apparent that crosslinking reactions disfavour the obtaining of a good molecular depth profile, while main-chain scission reactions (and in particular depolymerisation reactions, often referred as “unzipping”) are favourable for molecular depth profiling. In many cases both reaction pathways are possible and they are competing each other, although usually one of the two mechanisms is prevailing on the other.

Of course the particular behaviour of a certain polymer is strictly related with its structure and chemical reactivity, that influence the nature of the species (mostly radical species) produced by irradiation as well as their subsequent reactivity. It is not a simple task to identify the detailed reaction mechanisms involved in the degradation processes triggered by energetic particle irradiation. In many studied cases several elementary reactions (either consecutive or parallel) are invoked in order to explain the overall behaviour of a certain polymer. It is completely out of the scope of this Ph.D. work to enter in such a detailed description, that would imply the availability of a large amount of experimental information on the reaction intermediates, that is however not available. It is however possible, in a very simplified way, to sketch some general reaction steps that assume relevant importance in the ion beam induced modification of polymers. This can be useful in individuating some parameters that influence the experimental behaviour of polymers during nitric oxide assisted depth profiling of the the model polymers considered in the previous section.

In this simple and not exhaustive list of elementary steps, the detailed structure of the polymer is not considered, as we assumed that it is just a chain

where only C-C and C-H bonds are present. The presence of side chains and end groups is totally neglected. If P_n is a polymer with polymerization degree **n**, we assume that the events produced by the interaction can be only homolitic random chain scission or atomic hydrogen loss:

$$P_n \xrightarrow{\text{beam}} P_n^{\bullet} + H^{\bullet}$$

$$P_n \xrightarrow{\text{beam}} P_{n-q}^{\bullet} + P_q^{\bullet}$$

The above scheme implies only the generation of radicals: the production of ion pairs is neglected. Once they are produced, radicals will undergo several possible reactions. These can involve the conservation of a radical (radical propagation) or its disappearance (recombination or inhibition). Among the former kind of reactions we can consider:

1) radicalic depolymerisation (unzipping), where M is a monomer unit:

$$P_n^{\bullet} \longrightarrow P_{n-1}^{\bullet} + M$$

$$P_{n-1}^{\bullet} \longrightarrow P_{n-2}^{\bullet} + M$$

$$P_{n-2}^{\bullet} \longrightarrow P_{n-3}^{\bullet} + M$$

…

2) inter-chain radical transfer:

$$P_n^{\bullet} + P_m \longrightarrow P_n + P_m^{\bullet}$$

3) hydrogen abstraction:

$$P_n + H^{\bullet} \longrightarrow P_n^{\bullet} + H_2$$

The following reactions belong to the second group (recombination):

4) $P_n^{\bullet} + P_m^{\bullet} \longrightarrow P_{n+m}$

5) $P_n^{\bullet} + H^{\bullet} \longrightarrow P_n$

6) $H^{\bullet} + H^{\bullet} \longrightarrow H_2$

Finally, a particular case of radical recombination is the inhibition reaction that can occur in the presence of NO. This reaction is a well known one, as it has been exploited for titration of surface radicals in plasma-treated polymers[61 62]:

7) $P_n^{\bullet} + NO^{\bullet} \longrightarrow P_n\text{-}NO$

Once again it must be stressed that the scheme above outlined is a very simplified one. Nevertheless it contains some pathways that are relevant in characterising the behaviour of the model systems (PS and PMMA in particular) that we are considering. In particular, the propagating unzipping reactions (1) represent a paradigmatic decomposition pathway of type II polymers. It has been shown[63] that under polyatomic ion bombardment PMMA produces a substantial amount of monomer. On the other hand, the formation of new bonds (4) and loss of hydrogen (6) are characteristic of type I polymers. Polystyrene, in particular, is known to undergo, under ion irradiation, crosslinking[43-46] and loss of hydrogen[64].

It is commonly assumed that in real polymers both kind of pathways (chain scission and cross-linking) are present and competing each other, and that the observed behaviour is determined by the prevailing one. We note that the chain scission events are unimolecular (first order) reactions, while the recombination

elementary reactions, being bimolecular, are governed by second order kinetic laws, so that the concentration of radicals affects in different ways the reaction rates of these pathways. Keeping in mind these considerations, already in the simplified framework above outlined it is reasonable to expect that a change in the experimental conditions (temperature, average energy density delivered by an ion impact) can produce a change in the behaviour of a certain polymer, provided that the experimental parameters affect the radical concentration and the rate constants.

In this contest the addition of a radical inhibitor, such as nitric oxide, can affect the competition between unzipping and chain scission, at least for two reasons:

i) the decrease of active radical concentration produced by reaction (7) disfavours the second order reactions (such as crosslinking) with respect to the first order ones (like chain scission);

ii) it is reasonable to imagine also a spatial effect: while recombination reactions can be reasonably considered localised in the region where radicals are produced, the unzipping propagation reaction can easily “travel” along the length of a macromolecule (that can be much greater than the linear dimensions of the sample region energised by a single cluster impact), so subtracting the radical to the inhibiting effect of nitric oxide (that is estimated to be active only very close to surface) and “transporting” part of the active sites in peripheral regions or even outside of the collision cascade, where recombination reactions with other radicals are much less probable.

The above considerations can explain at least qualitatively the reason why the presence of NO dramatically affects the behaviour of PS while has little of no effect on PMMA. In this respect we must notice that some attempts have been made in order to quantify eventual small effects of NO dosing on the erosion yield of PMMA. We accumulated several depth profiles of PMMA and noticed that, in average, there is a small decrease (of the order of 10%) in the sputter yield of PMMA under C_{60} bombardment when nitric oxide is added. However such result can be affected by thickness inhomogeneities of the polymer film and by the uncertainty in the measurement of ion fluence, so that the question remains open.

Coming back to polystyrene, on which the effect of NO addition is dramatic, on the basis of the inhibition elementary reaction (7) we expect that NO should have some effect on the behaviour of this polymer under C_{60} irradiation.

In the following the main results of experiments conducted by varying p_{NO} are reported and discussed. Figure 18 reports, as function of NO partial pressure, the steady-state intensities of the signal $C_7H_7^+$, which is related with the polymer structure .

A clear trend is present in the plot. The intensity of the structure-related fragment increases until the maximum reached at p ~1.6×10^{-5} mbar

Generally speaking, an absolute intensity value of a certain peak in a SIMS spectrum cannot be directly related with the concentration at the surface of the corresponding species. This is due to a number of factors, among which the variation of the ionization probability due to changes in the chemical environment (matrix effect). This effect is well known in the case of oxygen dosing, that is

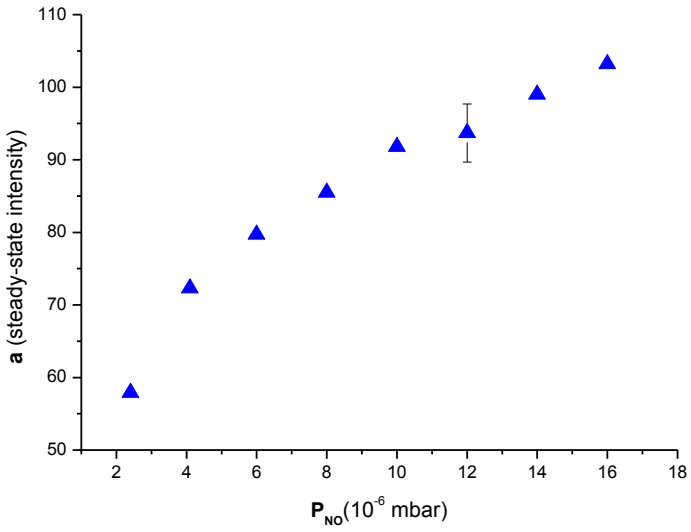

Fig. 18 – Intensities of the steady-state signal $C_7H_7^+$ of PS vs. P_{NO}

indeed exploited for increasing the positive ion yield. Some indication about the presence of such effect can be given by a normalization procedure. In our case we used the total ion intensity as normalization factor. Figure 19 reports, as function of NO partial pressure, the normalised intensities of two signals related with the pristine polymer structure (namely $C_7H_7^+$ and $C_8H_7^+$) as well as those of two signals (C^+ and CH^+) that are known to be related with the accumulation of damage (formation of new C-C bonds and hydrogen loss).

Two distinct trends are present in the plots. The intensity of structure-related fragments increases until a maximum is reached at p_{NO} ~1.0 x 10^{-5} mbar, and then tends to decay. Such a decay is probably connected with the fact that, by increasing the pressure in the analysis chamber, the transmission of secondary

ions is degraded and mass discrimination effects can be present due the increase of collisional events in gas phase, that are expected to affect more drastically secondary ions with larger mass with respect to low mass ones. At variance of the "molecular" fragments, the intensity of damage-related signals like C and CH decreases a monotonically with increasing pressure. The opposite trends shown by the two kind of peaks are a strong indication that the effect of NO is not (or at least not exclusively) that of a general increase of the ionization probabilities. Thus, the intensity increase of structure-related peaks and decrease of damage-related ones is a strong confirmation that the presence of nitric oxide reduces the damage accumulation and favours the emission of structure related ("molecular") fragments from the sample surface.

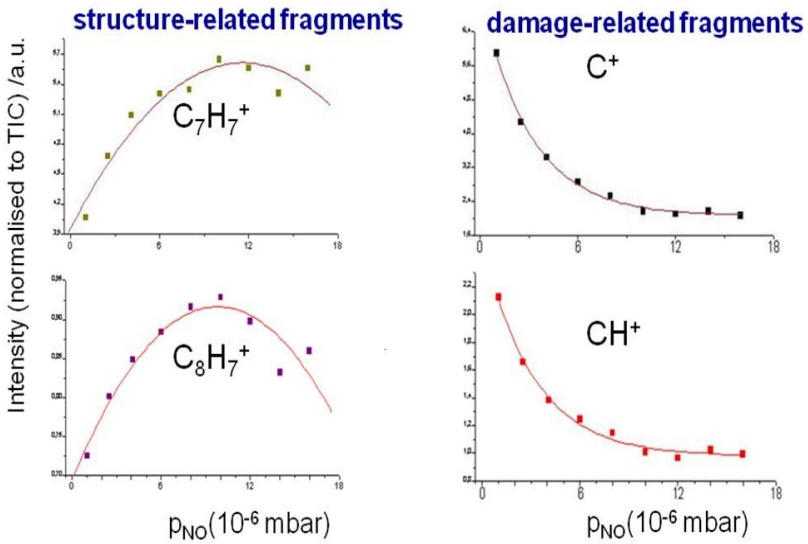

Fig. 19 – Intensities of structure-related (left) and damage –related (right) fragments of PS vs. P_{NO}

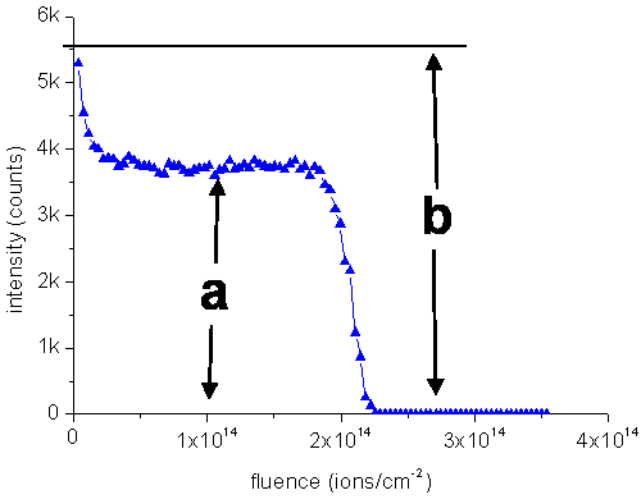

Fig. 20 – The steady-state intensity *a* compared with the initial intensity *b*.

According to Cheng et al.[65], the amount of accumulated damage can be estimated from the steady-state level of a certain secondary ion (SI) signal in a profile (see fig. 20). They define a "clean-up efficiency" based on two parameters, namely initial signal intensity *b* (approximately corresponding to that one would obtain in static SIMS conditions) and the steady-state intensity *a* that is attained in dynamic SIMS conditions if a successful depth profile is obtained. The lowering of the signal until the steady-state intensity is reached gives us a good indication of the amount of damage accumulation of a certain sample. If we assume that the a *a/b* ratio is a measure of efficiency of the damage removal at the steady state (i.e. the higher such a ratio the better the molecular profile), a unity value for the *a/b* ratio would indicate absence of damage, i.e. a perfectly ideal molecular depth

profile (like PMMA), while a zero value would indicate full damage (like PS in absence of NO).

In fig. 21 the dependency of the *a/b* ratio for the $C_7H_7^+$ signal of polystyrene on the partial pressure of nitric oxide is reported: an increase is observed, thus indicating a progressive lowering of damage with the increase of the partial pressure of NO.

Very interestingly, also the sputtering yield shows the same type of dependence on nitric oxide pressure (see fig. 22): the inhibition of cross-linking and the increased production of volatile species due to the enhancement of the chain-scission pathways (the same responsible for the high erosion yields of PMMA also in the absence of nitric oxide), can be considered responsible for the increase of sputtering yield.

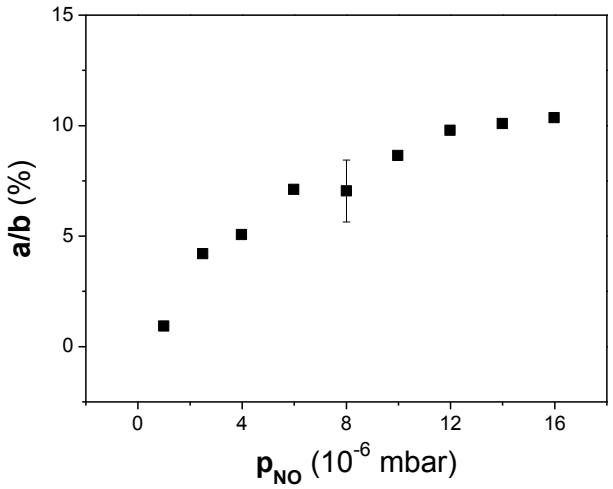

Fig. 21 - Damage lowering (a/b of $C_7H_7^+$ signal) vs. NO partial pressure.

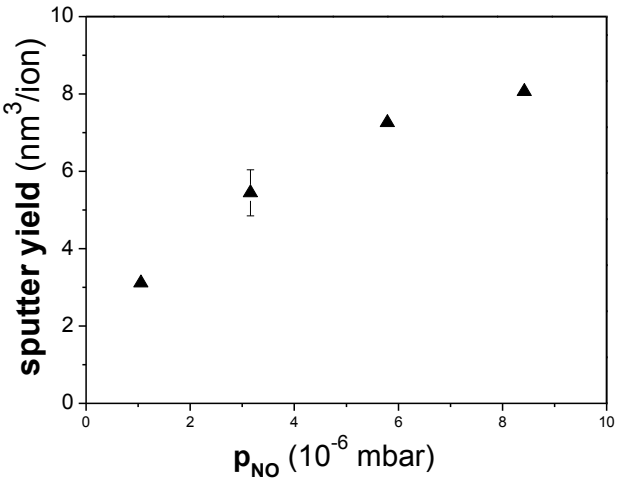

Fig. 22 - Sputter Yield of $C_7H_7^+$ signal vs. NO partial pressure

3.3 Multilayered systems

It is useful to remark the importance of the in-depth analysis in order to achieve information about the composition of inhomogeneous systems, especially those of industrial and technological interest, like layered structures, the basis of many molecular devices, organic/polymer-based, or even hybrid organic/inorganic systems. A certain number of studies are reported in literature about molecular depth profiling of multilayered systems, especially aimed to test the in-depth resolution of the cluster SIMS technique, thus a brief excursus is reported in the following, before starting with the discussion of the experimental obtained in this thesis work.

Wagner in 2005[66], by using 5 keV SF_5^+ as primary ion beam, investigated the in-depth resolution of moldel polymer-based multilayer made up by polymethylmethacrilate (PMMA), poly(2-hydroxyethylmethacrylate) (PHEMA), trifluoroacetic anhydride-derivatized poly(2-hydroxyethylmethacrylate) (TFAA-PHEMA), spin cast on silicon substrates. The author found that both the layered structure itself and the order of spin casting affect the erosion rate, wich is lower with respect to the single polymer layers. Observed effects during the analysis of this kind of material are the decrease in the sputter rate, due to a major damage accumulation in the overlayer, and an increase of the interface width with the depth. This effect is well known for inorganic systems, and it is due to the development of sputter-induced surface roughness. Cheng and Winograd in 2006[67] investigated hybrid multilayers made up alternate inorganic/organic (trehalose) on Si (using 20 keV C_{60}^+ primary ions). Results indicated the presence

of layer-by-layer interactions during the analysis, and beam-induced ion-mixing effects were also observed.

Zheng et al. in 2008[68] analysed Langmuir-Blodgett multilayers made up by arachidonic acid (AA) and dimiristoylphosphatidic acid (DMPA) using 40 keV C_{60}^+ ions. By acquiring depth profiles at liquid nitrogen temperature and room temperature, authors found that the intensities of the molecular signals remain constant in cryogenic conditions, while decrease of about 50% at room temperature, thus a minor damage accumulation occurring at low temperatures could be hypothesized. Furthermore, an increase of the depth resolution is observed at low temperature, thus indicating a thermal-induced ion mixing of the LB films. However, the explanation provided by authors for interpret the effects of temperature on molecular depth profiling, are often unconvincing and not valid in general. A recent study by Mao et al.[69] examined Δ-layers of Irganox 3114 intercalated between two thicker layers of Irganox 1010, using C_{60}^+ at 40 keV. Depth profiles were acquired in a range of temperature from 90 up to 300 K. The study demonstrates how, for the considered system, the depth resolution is negatively affected by the decrease of the average erosion rate, as well as the thermal-induced development of surface topography, occurring from 210 to 250 K. At lower temperatures, these thermal-induced processes appear to be deactivated, and constant values of depth resolution, erosion rate, intensity of molecular steady states are observed.

Niehuis et al.[70] used Ar_n (n = 500 to 5000) massive gas clusters to analyse OLED multilayered systems, finding that the sputtered volume increases at the increasing of the cluster size. Wehbe et al.[71] studied the performances of different cluster ions like Cs^+, C_{60}^+, Ar_n^+ (clusters quite different as energy per atom), in

depth profiling of an aminoacid-based multilayer. Authors found that the better performance is obtained by using the GCIB, despite its usefulness is limited for hybrid systems.

In conclusion, the molecular depth profiling of multilayers is affected by the nature of the considered layer and depending on the over-layer (X/Y is different from Y/X), thus a "normalization" effect, aimed to "uniform" different sputter yields and also to uniform the matrix effect, is required for the optimization of the molecular depth profiling of multilayered systems.

In the following, model polymer-based and hybrid polymer/inorganic multilayers experiment are described, in order to test the performance of the Nitric Oxide-assisted C_{60} SIMS technique in the case of multilayered systems, for future perspectives in depth analysis of materials of technological interest.

3.3.1 PS/PMMA/Si

In section 3.2 we have already examined the C_{60}-SIMS depth profiles of single layers of PS and PMMA on silicon, obtained both in UHV and in the presence of nitric oxide ($p_{NO}= 1.5\times10^{-5}$ mbar). In the following the experimental results obtained on layered polymer systems are shown. As already discussed, under C_{60} irradiation these polymers are paradigmatic of two opposite radiochemical behaviours, known as type I (in which cross-linking is the prevailing effect, as in PS under Ar^+ or C_{60}^+) and type II (in which the prevailing reactions lead to chain scission, as in PMMA under UV irradiation or C_{60}^+ - bombardment).

Looking at the C_{60} profiles of the single layers on Si (figures 3 and 10 for PS, 6 and 15 for PMMA), we observed that a successful molecular depth profile of PS is obtained only by using NO. Indeed structure related fragments can be observed (although with relatively low intensity) along the whole thickness of the sample. As pointed out previously, the effect of NO is that of inhibiting the ion-beam induced cross-linking that results in a progressive carbonization of the substrate with consequent loss of molecular information. The experimental results show also a tenfold increase of PS sputter rate in the presence of NO. By contrast, in the case of PMMA and other acrylates, it is known that successful depth profiling is possible (as shown in fig. 6) by simply replacing the monoatomic ion beam with a cluster primary beam (C_{60} or, with poorer results, SF_5^+). This is thought to be connected, in the experimental conditions of cluster-SIMS, to the prevalence of ion beam induced reactions leading to chain scission and formation of volatile species that are removed from the surface. Such release of volatile species limits the accumulation of chemical damage at the "new" surface left behind by the sputtering process, thus allowing in-depth characterization of the polymer. We also observe that the presence of NO has a negligible effect on the quality of PMMA depth profile, if one excludes the interfacial region with silicon substrate (fig. 13), and virtually no effect on the sputtering rate. This is not unexpected because, as discussed before, nitric oxide is expected to be more effective in inhibiting the second order cross-linking reactions rather than the first order chain scission reactions, that, moreover, are often chain reaction so that they need just a small concentration of initiating radical sites for producing a high amount of volatile products.

The experimental results on single polymer films suggest that NO has an "uniforming" effect on the sputtering behaviour (under C_{60}) of polymers that otherwise behave in opposite way. This prompted us to investigate layered systems, containing polymers with different radiochemical behaviour under cluster irradiation. We started with the most simple case, i.e. a bi-layer PS/PMMA on silicon.

As expected, such a system cannot be satisfactorily profiled in the absence of NO, due to the type I behaviour of the outermost PS layer. However, the situation changes in the presence of NO, as demonstrated by the depth profile of fig. 23, were the two different layers are clearly distinguished. The time required for sputtering each layer (both of comparable thickness) is comparable for both layers, confirming the leveling effect of NO on the sputter yield. It is worth to note that the overall intensity of fragments (not only those reported in figure) is much lower in the PS layer than in the PMMA layer. As a result, the intensity of fragments that are distinctive of polystyrene (such as those at 91, 103 and 115 u), but are also present in PMMA as minor fragments, appear to be higher in PMMA than in PS itself. However such somewhat casual occurrence does not prevent to recognize the chemical identity of the two layers, as the full spectra reconstructed from the two regions of the profile are very similar to the static SIMS spectra of PS and PMMA respectively.

Another useful information coming from the depth profile of fig. 23 is the behaviour of the unspecific C^+ signal (black), in countertrend with respect to the structure-related signals of polymers. Such signal, that can be considered a sort of signature of the accumulation of damage, is comparatively much more intense in polystyrene than in polymethylmetacrylate indicating that, although limited by the

presence of nitric oxide, the accumulation of damage is more pronounced in PS than in PMMA.

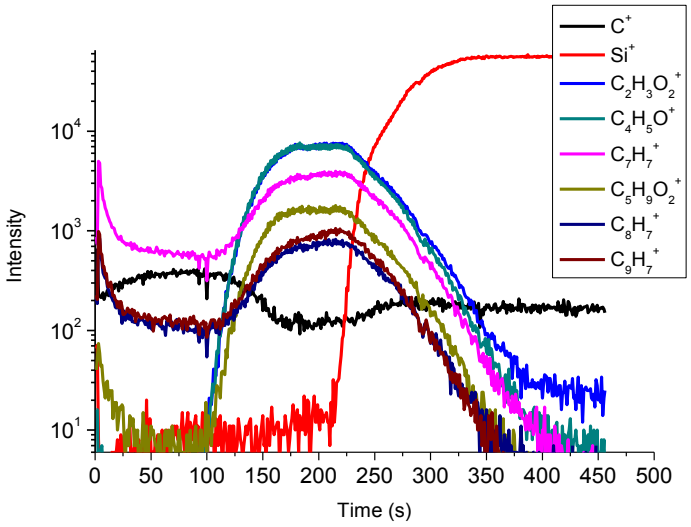

Fig. 23 - C_{60} depth profile of the PS/PMMA/Si multilayer, with NO $1.5x10^{-5}$ mbar.

3.3.2 PS/PMMA/PAA/PETi/Si

This system has been devised with the aim of testing the capability of NO-assisted C_{60}-SIMS in discriminating among different layers in complex systems. In particular two type II polymers of very similar behaviour, composition and structure (PMMA and PAA) are sandwiched between two layers, PS and polyethylene terephthalate-co-isophthalate (PETi), for both of which a large

prevalence of damage accumulation* is observed. Moreover, the elemental composition of PETi is very close to that of PMMA. The experimental depth profiles are reported in fig. 24 (without NO) and in fig. 25 (with p_{NO} ~10^{-5} mbar). It must be noted that the profile of figure 24 has been obtained with a C_{60}^+ current density ~3 times higher than that used for the profile in presence of NO. This in order to avoid beam stability problems connected with the very long sputtering times needed for profiling the whole thickness of the sample in the absence of NO.

The profile obtained without NO-dosing is characterized – as expected - by the absence of structure-related ("molecular") signals from the PS and PETi regions, where only aspecific fragments, such as C^+, are detected. Molecular signals are obtained only from the acrylic layers, but PMMA and PAA are not clearly discriminated each other. Furthermore, it must be observed that, although the fullerene ion fluence delivered to the sample during the whole experiment is ~6 times higher than that used in the profile of fig. 25 (with NO), the interface with silicon is not reached within the measurement time. This behaviour is indicative of massive build-up of damage in the polyester layer, that causes a decrease of the sputter yield and presumably some accumulation of carbon from the fullerene beam. In any case, as expected, this experiment confirms that with C_{60} beams it is not possible to obtain reasonable molecular depth profiles from multilayers containing type I polymers..

The situation changes quite dramatically with the introduction of nitric oxide in the vacuum system during the analysis, as shown in fig. 25. Indeed we note that: i) "molecular" fragments are detected from all the layers; ii) all layers are

* The single-layer behaviour of PETi will be discussed later in the next section.

clearly discriminated, although some fragments are present in more than one layer; iii) all the layers are sputtered with comparable rate and iv) the interface with silicon is clearly reached. In other words, we can consider the profile of figure 25 as a successful molecular depth profile.

Interestingly, by monitoring the carbon signal, we can observe, in analogy with the case of the simpler PS/PMMA system, that its intensity is not constant along the different layers, but it is higher in those layers (PS and PETi) where we expect a larger amount of damage accumulation.

A closer inspection of the profile of figure 25 reveals other features. In particular, the signal intensities at the interfaces show in some instances (see for example the $C_4H_5O^+$ fragment of PMMA) the presence of peaks that are unlike to be related with concentration fluctuations. This is not uncommon and, in analogy with inorganic depth profiles, it can be ascribed either to changes of sputter rate at the interface between two different materials or to a change in the ionization probability (matrix effect).

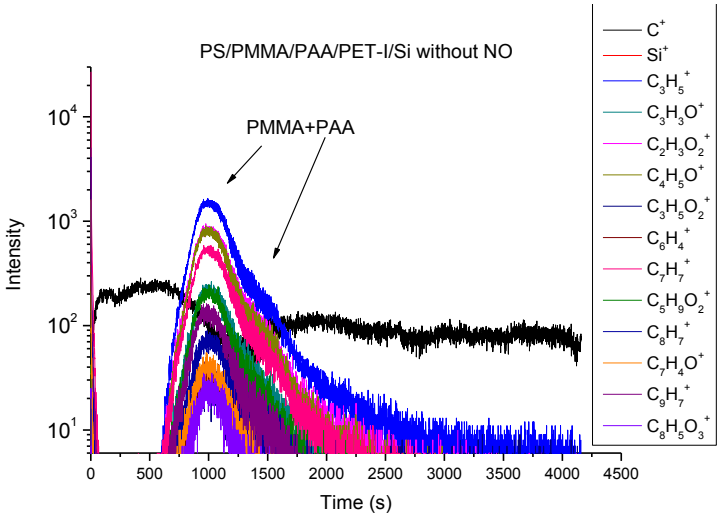

Fig. 24 - C_{60} depth profile of the PS/PMMA/PAA/PETi/Si multilayer, without NO

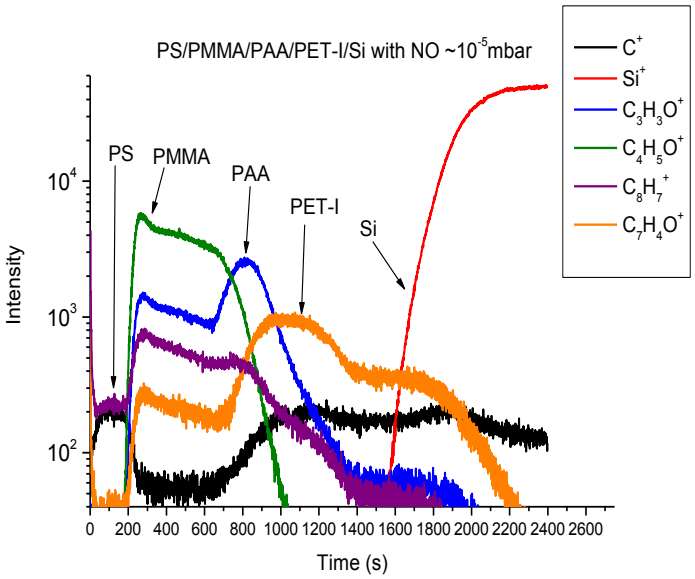

Fig. 25 - C_{60} depth profile of the PS/PMMA/PAA/PETi/Si multilayer, with NO ~10^{-5} mbar.

3.3.3 Hybrid multilayers

As outlined in the introduction, one of the present challenges in SIMS depth profiling is that of obtaining molecular depth profiles from polymer (organic) systems without losing the ability to sputter inorganic materials. This is relevant in the characterization of multilayers of technological interest, as well as of composite and hybrid systems, where strong differences in sputtering rate would render problematic or even impossible either the measurement or the interpretation of depth profiles and 3D images. In the following we report the results obtained on some hybrid model multilayers, containing alternate polymer

and inorganic (gold) layers. The aim is that of giving a proof-of-concept of the capabilities of NO-assisted C_{60}-SIMS in the characterization of complex hybrid systems.

The first multilayer we consider consists of an outer layer of polystyrene (PS), separated by an Au layer deposited on top of a PMMA film in turn spin cast onto a polyethylene terephthalate (PET) plate. The PMMA layer was doped with cobalt acetate in order to have an additional inorganic marker available for that layer. Of course C_{60}-SIMS depth profiles were measured in the presence of nitric oxide, on the basis that neither PS nor PET molecular signals has been retained in its absence in the profile of fig.24.

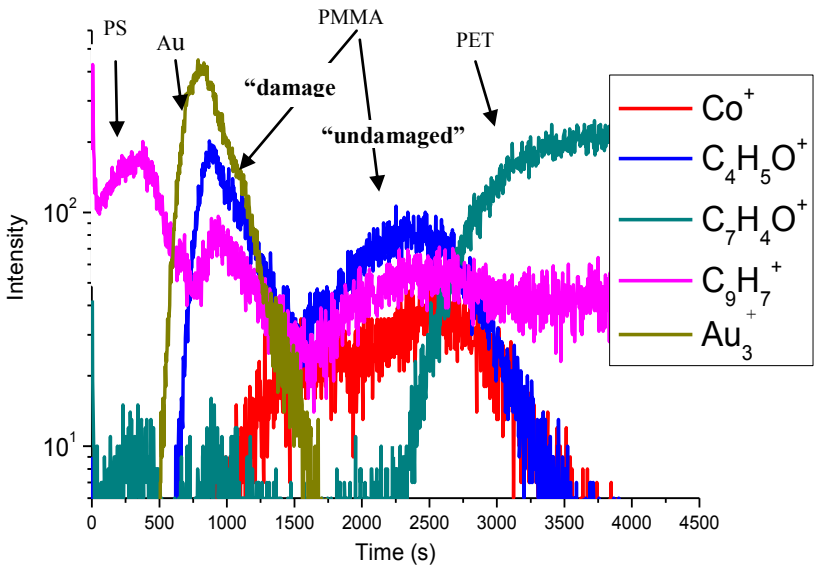

Fig. 26 - C_{60} depth profile of PS/Au/PMMA(Co)/PET multilayer with NO ~10^{-5} mbar.

The first observation from the profile of this system, reported in fig. 26, is that all the layers are profiled down to the substrate and each layer can be distinguished from the others. In the first part the molecular signals of PS are retained until the interface with Au is reached. The gold layer is sputtered away (as shown by the evolution of Au_3 signal) and after it the PMMA layer is profiled down to the PET substrate that is identified as well. The evolution of the signals in correspondence of the PMMA layer deserves some further comment. Indeed, a region of overlap of Au and PMMA signals is observed, followed by a decrease and then a rise of the PMMA-related signal. The overlap region is probably due to the presence of a damaged PMMA region were gold is diffused. This damaged region is most likely produced during the sputter deposition of the gold layer, that implies the irradiation of the underlying PMMA film with energetic species (ions, electrons, photons). Interestingly, the cobalt, used as a marker of PMMA, is absent from the gold-containing region and intensity of the Co^+ signals closely follows the behaviour of $C_4H_5O^+$ in the inner (most likely undamaged) part of PMMA.

Another explanation could be that of beam-induced damage of the interface during the analysis. This effect is known in literature, and in the case of other hybrid systems like trehalose covered by silver a similar effect was observed[13] and it was supposed to be generated by a recoil of the metal, or by emission of secondary electrons from the metal layer, induced by the bombardment with C_{60}.

A further example of hybrid multilayer is the PS/Au/PMMA(Co)/Au/PETi/Si system. The depth profile of this complex system is reported in fig.27. Also in this profile each layer can be clearly discriminated. Moreover, the sputtering rate of

each layer appears to be of the same order of magnitude, in spite of the large differences in the nature of the layers. The above observations allow to state that, as the previous one, the profile of figure 27 can be considered an example of successful depth profile, although, again, the PMMA layer suffers some damage effect. Among the adverse effects that deserve further investigations, a rapid degradation of depth resolution as function of depth must be noticed, as shown by the longer tail of the inner gold layer compared with that of the outer one. This is a quite well known problem in depth profiling, and usually it arises mainly from the development of surface topography in the sputter crater bottom (provided that crater edge effect are not present). Such effect can be minimized, for example, by sample rotation during sputtering. However, in spite of some evident limitation in the quality of the profiles of the hybrid multilayers presented here, it must be remarked that they represent the first proof-of-concept of the applicability of the NO-assisted C_{60}-SIMS to the characterization of complex hybrid polymer/inorganic multilayers, that are expected to be difficult to profile even with the novel GCIBs.

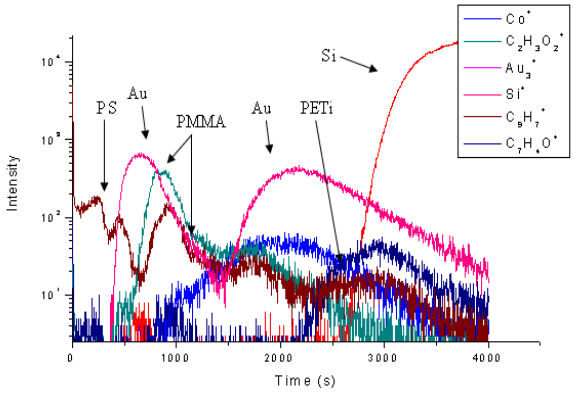

Fig.27 - C_{60} depth profile of PS/Au/PMMA(Co)/Au/PETi/Si with NO ~10^{-5} mbar.

3.4 Other polymer-based systems

As mentioned in the outlined, we decided to extend the application of the NO-assisted C_{60} depth profiling to more complex systems, in which polymer materials with different nominal behaviour (type I vs. type II) do co-exist, either in the same macromolecule, as in the case of styrene-methylmethacrylate random copolymers (3.4.1), or in the same material, like immiscible polymer blends (3.4.2), such as PS/PMMA and PC/PET.* Finally, a short presentation of some results on additive-containing polymer systems is also reported (3.4.3).

3.4.1 Random copolymers

The investigation of this type of material is thought to be useful in investigating the role of nitric oxide dosing during depth profiling with C_{60} primary ions in copolymer systems containing different proportions of the two monomers that, in the respective homopolymers, give rise to materials with different behaviour with respect to C_{60} cluster-SIMS. In particular, we studied styrene-methylmethacrylate copolymers, in order to compare their behaviour with that of the two homopolymers (PS and PMMA, respectively type I and type II) already discussed previously. Three different MMA/Styrene ratios have been considered, and the depth profiles obtained both with or without the introduction of nitric oxide during the measurement are presented in order of increasing content of styrene.

* the behaviour of the two pure PC and PET polymers will be reported as well.

Figs. 28 and 29 show the depth profiles of a copolymer containing only 8% of styrene, obtained without and with NO dosing respectively. Such system behaves pretty similarly to the methylmetacrylate homopolymer: indeed both in absence and in presence of NO a successful molecular depth profile is obtained and the effect of NO is negligible, with no influence on the erosion rate or in the secondary ion intensities. Interestingly, also the ratios between MMA- and Styrene-related peaks (both observed in the profiles) are not affected by the presence of NO. We can hypothesize that the presence of a relatively small amount of styrene units in the chain does not affect the overall radiochemical behaviour of the system, that maintains the type II behaviour of pure PMMA. As already observed in the case of PMMA, the only appreciable effect of NO is noticed at the interface with silicon, where it induces an enhancement of the silicon signal and a flattening of the ionization yield of the interfacial silicon oxide and of the inner elemental silicon. This effect is very similar to that produced by oxygen dosing in depth profiling of inorganic materials, that is used in order to level-out the strong differences in ionization probabilities among elements and their oxides.

As one could expect, the situation changes as the content of styrene units increases in the copolymer. The results obtained on a random copolymer with 1:1 styrene/methylmethacrylate ratio are reported in figs. 30-31.

In the case of the profile acquired in absence of NO (fig.12), the intensity of structure-related signals falls down of more than three orders of magnitude as soon as the static limit is trespassed, although some residual intensity is

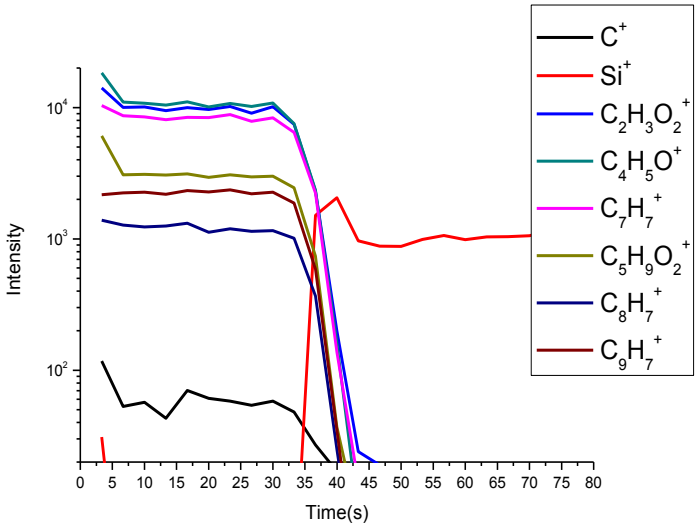

Fig. 28 - C_{60} depth profile of Styrene 8%-MMA 92% copolymer, without NO.

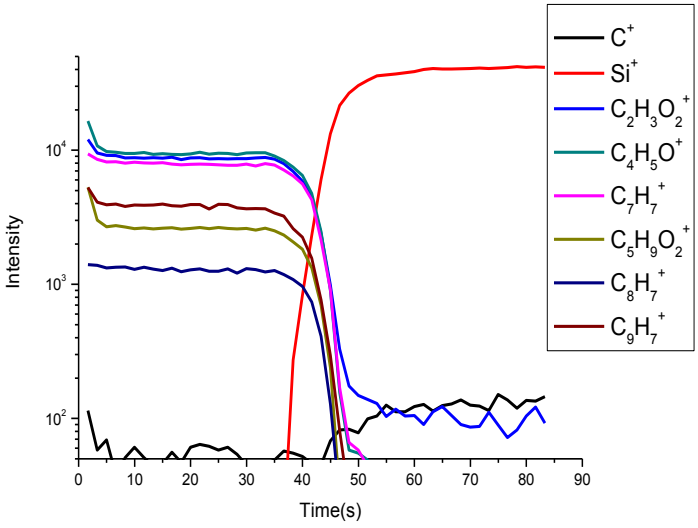

Fig. 29 - C_{60} depth profile of Styrene 8%-MMA 92% copolymer, with NO ~10^{-5} mbar.

maintained above the noise level. Parallel to this decrease, a noticeable build-up of C^+ intensity is observed, confirming that a substantial accumulation of damage is occurring. After about 1 hour of sputtering (in the experimental condition used) the silicon interface is reached, with a quite poor depth resolution. In other words, in the 1:1 styrene-MMA random copolymer, the type I behaviour of polystyrene appears to be the prevailing one in spite of the 50% of MMA units randomly distributed in the polymer chain. Such behaviour is easily understood by considering that the unzipping reactions (i.e. the self-propagating depolimerization radical reactions) that are thought to characterize the PMMA behaviour under fullerene irradiation, are suppressed (or at least greatly limited) by the presence of styrene units that are intercalating (statistically in a 1 to 1 ratio) the MMA units, so that the competing cross-linking reactions, characteristic of polystyrene but present also in polymethylmetacrylate, become the prevailing reactions.

By addition of NO, however, the situation is sensibly changed. As shown in fig. 31, there is larger retention of both styrene- and MMA-related fragments along the film depth (compared to the case of fig. 30), although their intensity decays without reaching a steady state, indicating a certain accumulation of damage. The beneficial effect of NO is also reflected in the sputter yield: indeed, with the same beam current density (and of course the same film thickness), the interface with silicon substrate is reached in about ~300 s, i.e. there is an increase of one order of magnitude in the sputtering yield produced by NO dosing.

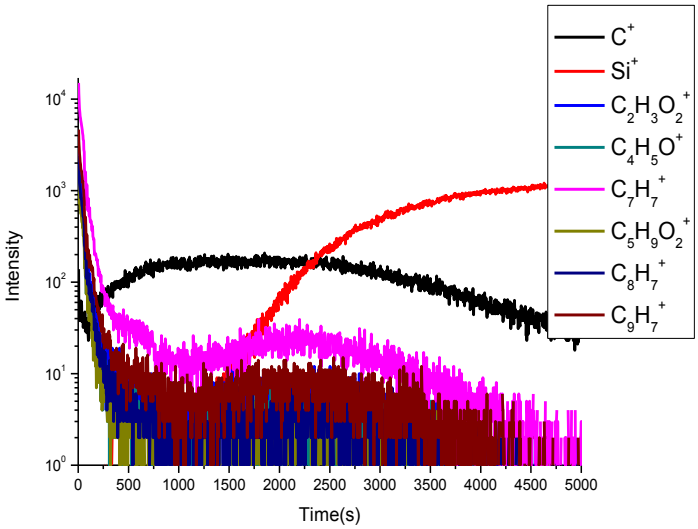

Fig. 30 - C_{60} depth profile of Styrene 51%-MMA 49% copolymer, without NO.

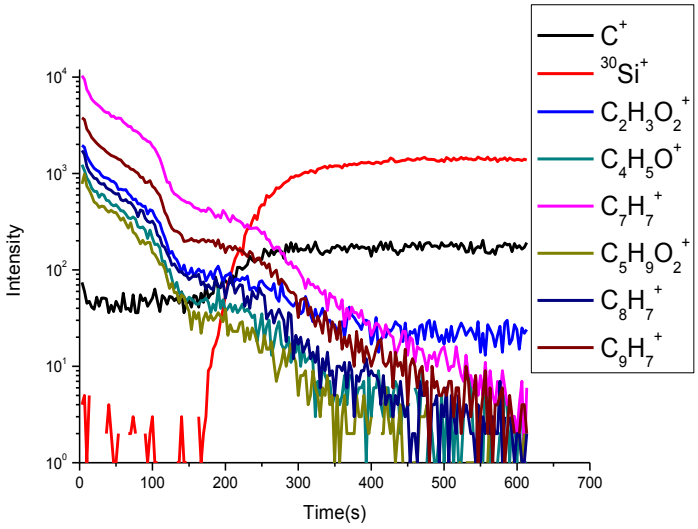

Fig. 31 - C_{60} depth profile of the same sample of fig. 30 (styrene 51%-MMA 49% copolymer), but with NO ~10^{-5}mbar.

Finally, figures 32-33 report the depth profiles of a random copolymer with prevailing amount of styrene (91% Styrene/9% MMA). Not unexpectedly, in view of the statistical presence of relatively large polystyrene blocks in the chain, this copolymer behaves, under fullerene irradiation, in a way similar to that of polystyrene (see figure 32 in comparison with fig. 3). The NO dosing, again as in the case of pure polystyrene, allows to obtain a certain degree of molecular information along the film depth (see figure 33 in comparison with fig. 10) and, at the same time, causes an increase of the sputtering yield.

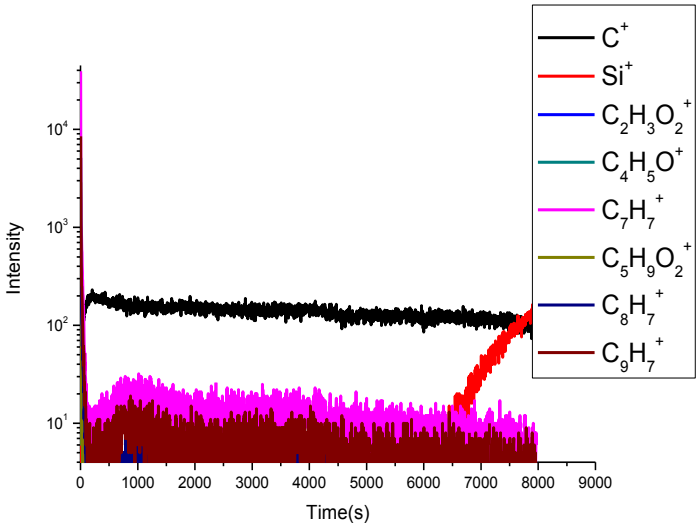

Fig. 32 - C_{60} depth profile of S 91%-MMA 9% copolymer, without NO.

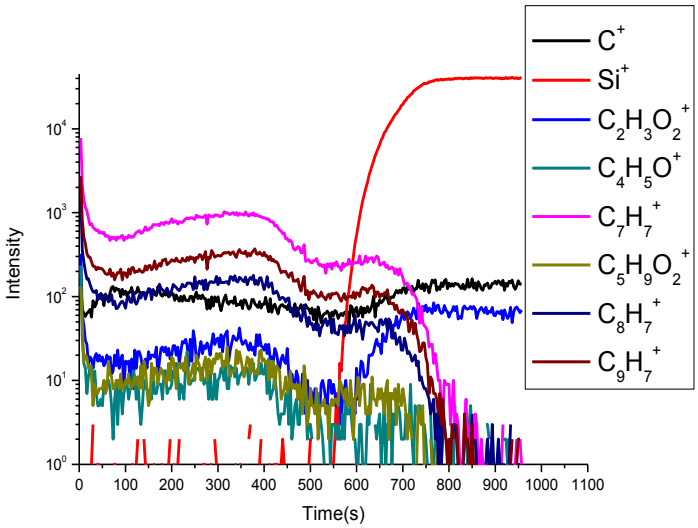

Fig. 33 - C_{60} depth profile of S 91%-MMA 9% copolymer, with NO ~10^{-5}mbar.

3.4.2 Immiscible polymer blends

Another interesting type of complex polymer sample is represented by immiscible polymer blends that, upon deposition from homogeneous solution give rise to phase separation. The presence of domains of different phases with different behaviour under ion beam irradiation makes the spatially resolved compositional characterization of such systems a quite challenging task, since the different domains not only give rise to different ion intensities but also exhibit different sputtering rates (so producing uneven advancing of the crater bottom surface during sputtering) and can accumulate ion-beam induced damage in different degree, from type I to type II behaviour with a range of intermediate

behaviours. The systems chosen for our investigation are two immiscible polymer blends, in particular PS/PMMA and polyethylene terephthalate / bisphenol A-polycarbonate (PET/PC). The choice of the first blend is straightforward, since the two component polymers exhibit opposite behaviour, as largely discussed in the previous sections of this work. The PET/PC blend has been chosen because this system is largely studied (for example it is known to undergo complex thermal compatibilization reactions[72, 73]) and because of the interesting properties and the technological applications of the two corresponding homopolymers. Moreover, under fullerene irradiation PET is reported to display a partial type II behaviour while polycarbonate exhibits a type I behaviour. The composition of the blends (4:1 w/w for PS/PMMA and 3:1 w/w for PC/PET) have been chosen in order to make comparable the secondary ion intensities of each component in the static SIMS spectrum. In fact, it is well known that, in the same experimental conditions, the total ion intensities of PMMA and PET are much more intense than those of PS and PC, respectively.

At variance of the polymer systems discussed in the previous sections, that are characterized by a uniform lateral composition (i.e along each of the planes parallel to the surface) immiscible polymer blends, due to phase separation, are characterized by 3D compositional inhomogeneity, that can be evidenced at the surface by means of resolved chemical maps (ToF-SIMS imaging), as shown in fig. 34 for PET/PC and fig. 35 for PS/PMMA. These images are obtained by reporting the intensity distribution (rendered in a colour scale) of a selected fragment present in the spectrum. Due to the parallel acquisition in the ToF analyzer, it is possible to obtain a map for each peak present in the spectrum. Actually the maps reported in the following have been obtained summing up the

intensities of the distinctive fragments of each polymer in the blend and then overlaying the two distributions by attributing a different colour to the signals of the two polymers in the blend. In both images, obtained in static SIMS mode by using a focused bismuth beam, the phase separation is clearly evidenced.

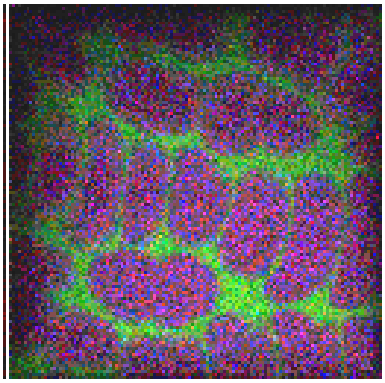

Fig. 34 - False-colour image overlay of a PC/PET blend 3:1. Purple=PC, Green=PET. Field of view 500µm×500µm.

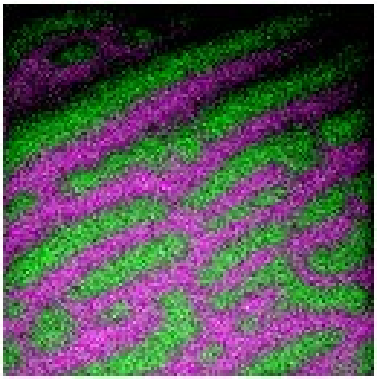

Fig. 35 - False-colour image overlay of a PS/PMMA blend 4:1. Purple=PMMA, Green=PS. Field of view 500µm×500µm.

In order to obtain a full 3D characterization one should couple the 2D imaging capabilities of the focused ion-beam with an in-depth analysis. In principle this should be easily obtained in dual ion beam mode, by exploiting the characteristic of cluster beams in for molecular depth profiling joined with the high lateral resolution of focused ion beams. It must be pointed out that, at the present stage, it was impossible to obtain satisfactory 3D images, mainly due to limitations imposed, in the experimental apparatus used, by a low signal-to-noise ratio that degrades the lateral resolution. However we obtained interesting evidences on the applicability of NO-assisted C_{60}-SIMS in this direction, by studying the depth profiling of the immiscible blends, although without sufficient lateral resolution.

3.4.2.1 PS/PMMA 4:1 blend – Depth profiling

As clearly shown in fig. 36, the depth profile of the PS/PMMA blend obtained in the absence of NO is very similar to that of pure PS, i.e. completely unsatisfactory, with a rapid decay of molecular signals at the early stages of the erosion. By contrast, by introducing NO in the analysis chamber (fig. 37), molecular signals are retained along the profile down to the interface. This is a promising finding in view of the development of 3D characterization. The presence of two distinct plateau regions in the profile is not completely understood. One could speculate that it is due to the different sputter rates of the two different types of domains (PS and PMMA) that causes the earlier reaching of the silicon interface in the regions covered by the polymer with higher sputter rate,

presumably PMMA. However further investigations are needed in order to elucidate this point.

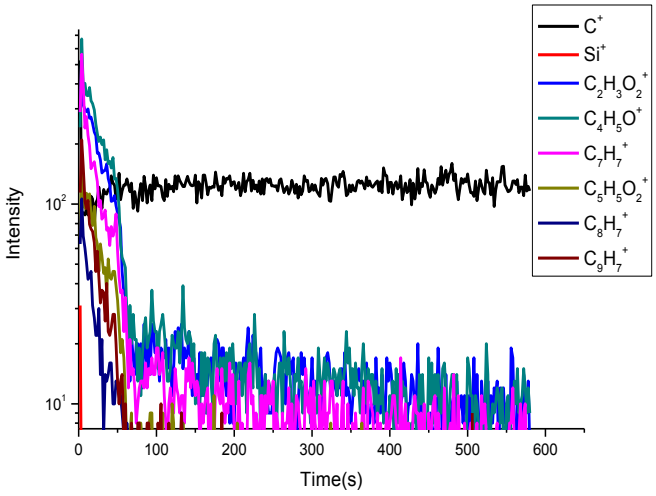

Fig. 36 - C_{60} depth profile of PS/PMMA blend 4:1, without NO.

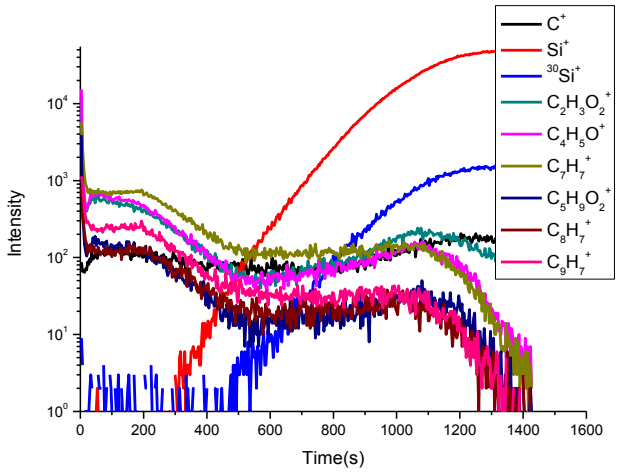

Fig. 37 - C_{60} depth profile of PS/PMMA blend 4:1, with NO ~10^{-5} mbar.

Before starting the discussion about the immiscible blends made up by polyethylene terephthalate (PET) and bisphenol-A-polycarbonate (PC), it is useful to make a brief digression about the fullerene SIMS depth profiling of each homopolymer.

3.4.2.2 Polycarbonate (PC)

Bisphenol A-polycarbonate is widely used in various technological applications, due to its peculiar properties (e.g. durability, transparecy). However, from a chemical point of view, this polymer belongs to the type I behaviour category, undergoing mainly ion beam-induced crosslinking process when irradiated. Despite it has been recently reported that PC can be profiled by using low energy Cs primary ions[74], or by grazing incidence of 76° of C_{60} bombardment[75], however it cannot be profiled with fullerene in standard geometry experiments. Then the nitric oxide dosing has been extended to the investigation of polycarbonate, and results indicate that the use of nitric oxide works also for this polymer, as it can be seen in the following figures:

In figure 38 is reported the "classical" fullerene depth profile of PC. No molecular signal is retained, as they rapidly drop to zero, and a very low erosion rate is observed. In fig. 39 and 40 the depth profiles acquired in presence of nitric oxide (~1.5 x 10^{-5} mbar) are reported, and they show evidence of strong improvements: the obtaining of molecular depth profiles and enhanced erosion

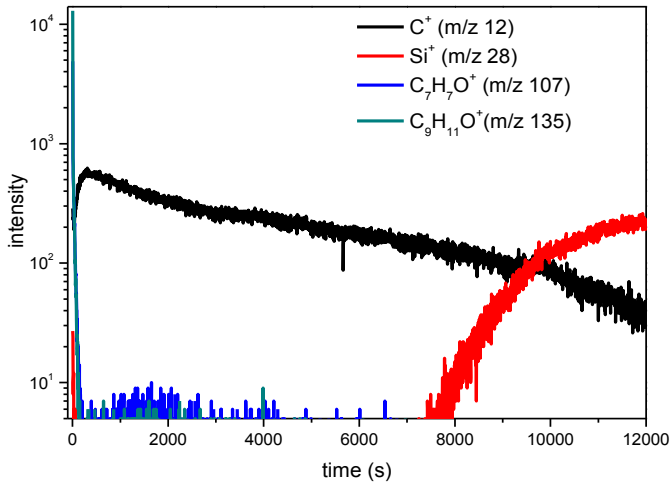

Fig. 38 - C_{60} Depth profiling of PC in absence of NO dosing

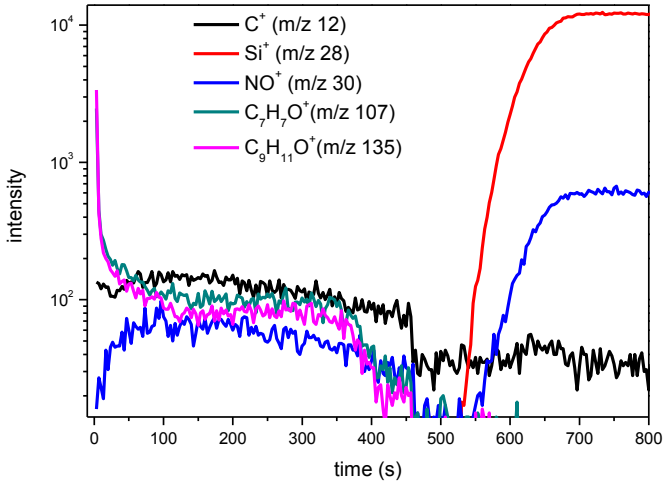

Fig. 39 - C_{60} Depth profiling of PC with NO 1.5 x 10^{-5} mbar, positive ions

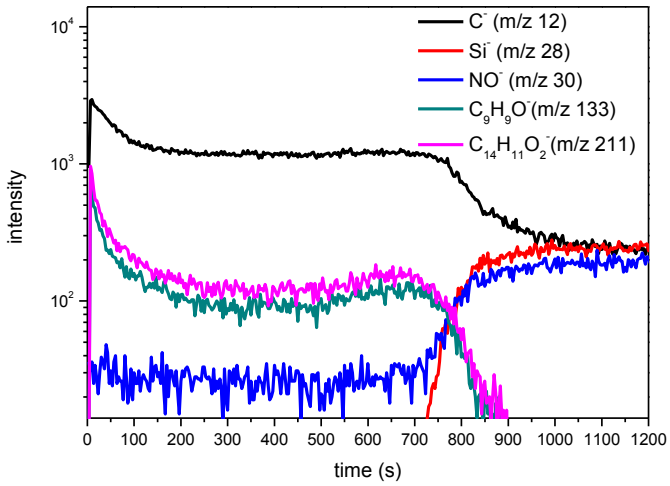

Fig. 40 - C_{60} Depth profiling of PC with NO 1.5 x 10^{-5} mbar, negative ions

rates (more than 10 times). Furthermore, the dynamic SIMS spectra, reconstructed from the steady state region of the profiles are similar to those acquired under the static limit (positive and negative, see and compare fig. 41 with fig. 42 and fig. 43 with fig. 44). This indicates, in analogy to PS and PAMS, an efficient role of nitric oxide as a species able to reduce the accumulation of damage.

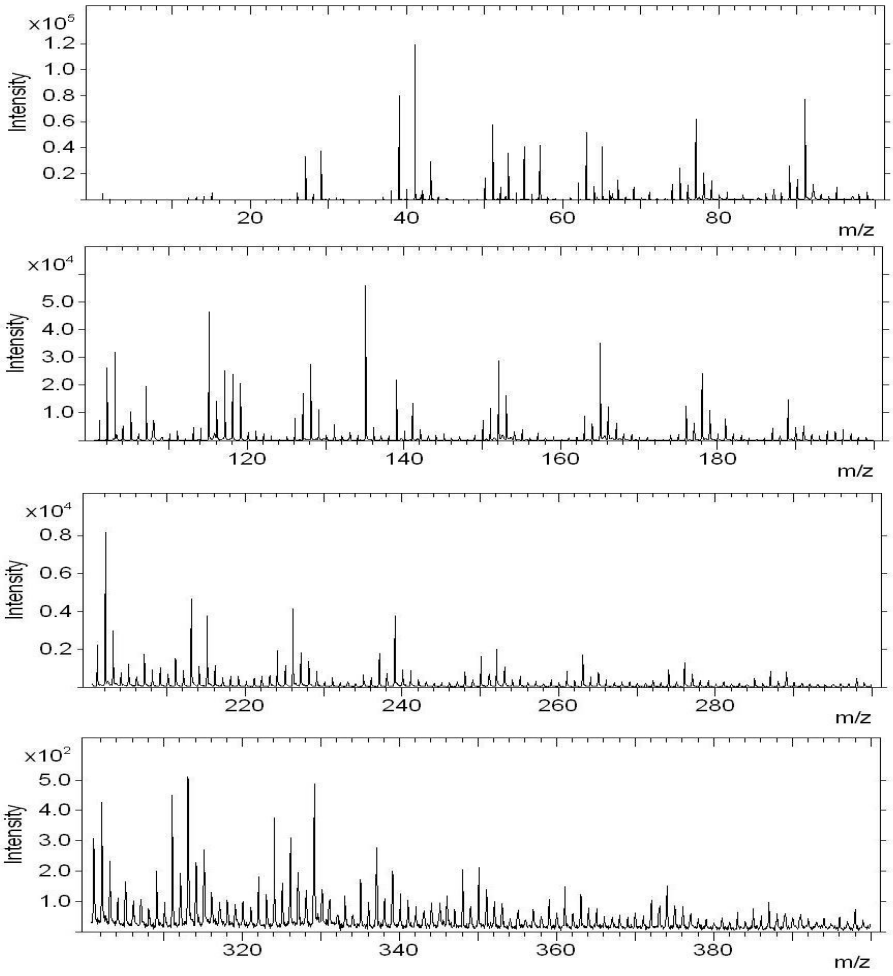

Fig. 41 - Positive ion static SIMS spectrum of PC

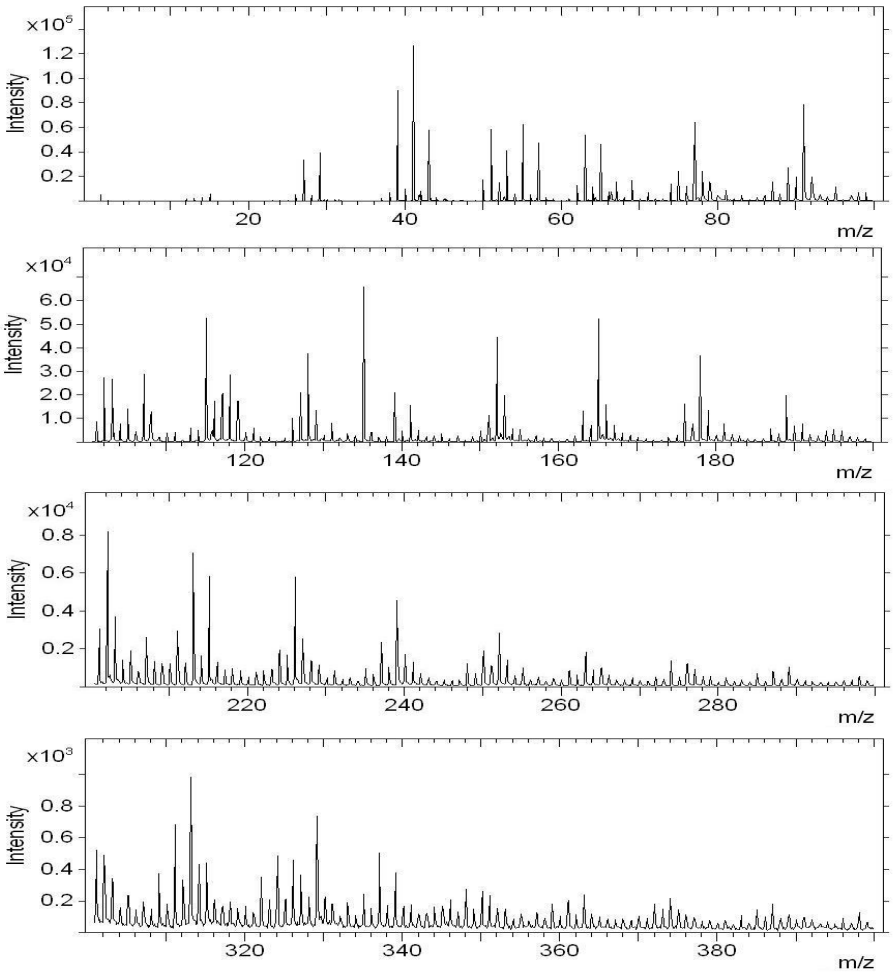

Fig. 42 - Positive ion dynamic NO-assisted SIMS spectrum of PC (reconstructed from the steady-state region).

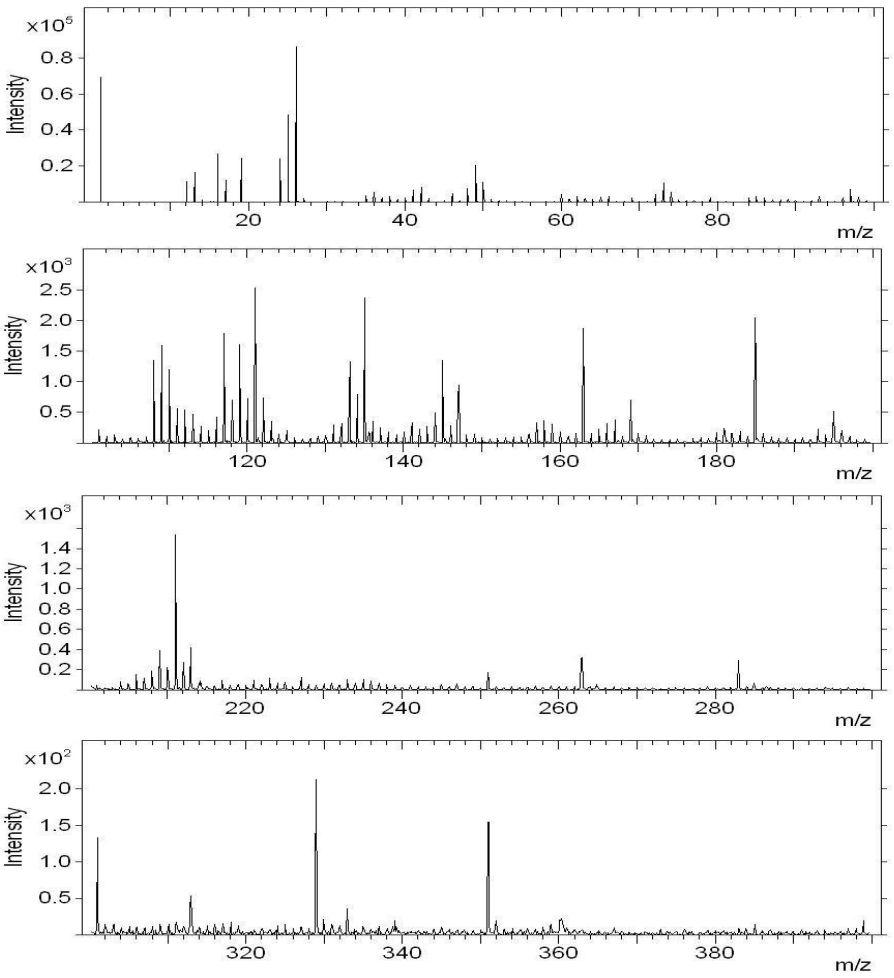

Fig.43 - Negative ion static SIMS spectrum of PC.

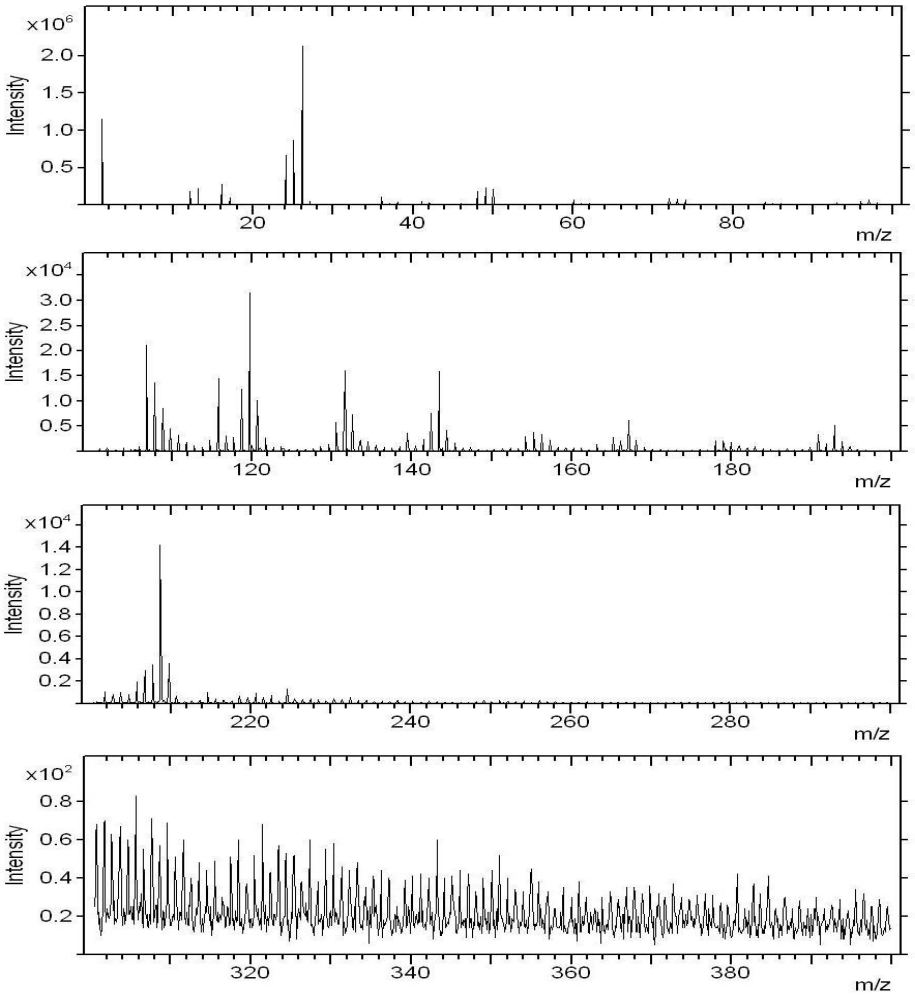

Fig. 44 - Negative ion dynamic NO-assisted SIMS spectrum of PC (reconstructed from the steady-state region).

3.4.2.3 Polyethylene terephthalate (PET) and polyethylene terephthalate-co-isophthalate (PETi)

In order to investigate the behaviour of this polymer, the amorphous analogous of PET, polyethylene terephthalate-co-isophthalate (PETi) was analysed, because of its better characteristics in terms of solubility and because it easily forms (at variance of the highly crystalline PET) homogeneous films when prepared *via* spin coating. In fig.45 the C_{60} depth profile in absence of NO is reported: we can observe a behaviour in some aspects similar to that of polyacrylates (tendency to type II behaviour), although some damage accumulation cannot be neglected. Also, a peculiar "slope" of the profile can be noted, that indicates a "quasi-successful" molecular depth profile. Anyway, this behaviour is still very different from that of PC, despite the chemical structure of both polymers is made up by ester functional groups and both system contain

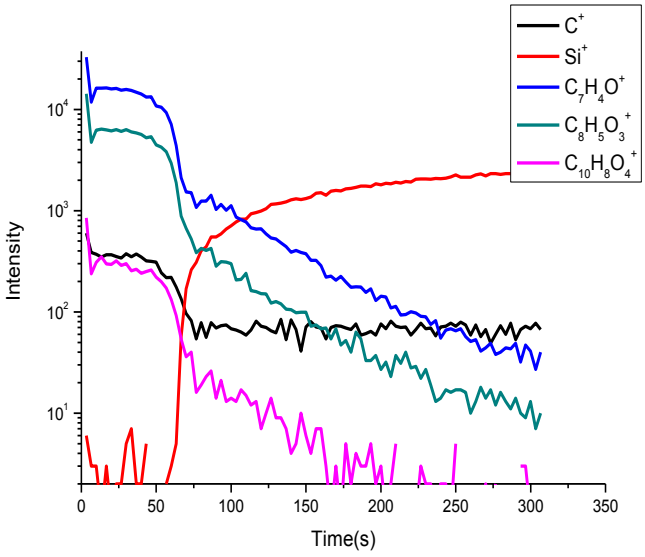

Fig.45 - Depth profiling of PETi in absence of NO.

aromatic rings in their main chain. The effect of NO (see figure 46), although not so spectacular as in other cases, is that of improving the type II behaviour of PETi, making it more similar to that of PMMA, without strong effects on sputtering rate.

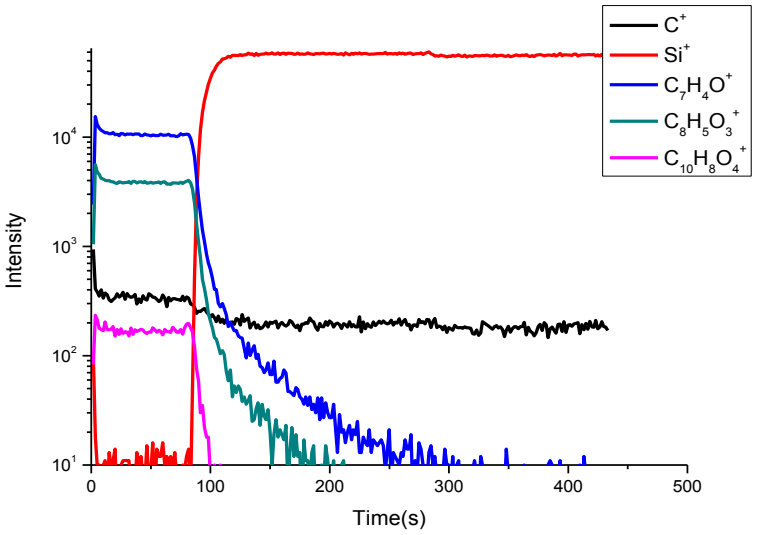

Fig. 46 - Depth profiling of PETi with NO-dosing

3.4.2.4 PC/PET 3:1 blend – Depth profiling

Analogous measurements of the PS/PMMA blend film were performed on the PET/PC one. It must be noted that while PET (and his amorphous analogous

PETi) is reported to be amenable of depth profiling with fullerene beams (although with a non-negligible damage accumulation), PC shows a typical type I behaviour, that however is converted to type II in the presence of NO (see figures 38, 39 and 40). When profiling the PET/PC blend in absence of NO (fig.47), as observed in the case of PS/PMMA the dominating behaviour is that of the type I component, that causes accumulation of damage and prevents the observation of structure-related fragments along the depth. The introduction of NO, also in this case, allows to obtain a molecular depth profile (fig. 48), with the retention of molecular signals and increase of more than one order of magnitude of the sputter rate (compare the timescales in abscissa in figs 47 and 48). Again, the role of NO in reducing ion beam induced damage and in uniforming the sputter behaviour of different polymers even in complex systems is confirmed and this candidates NO-assisted C_{60}-SIMS as a possible tool for 3D imaging of polymer-based systems.

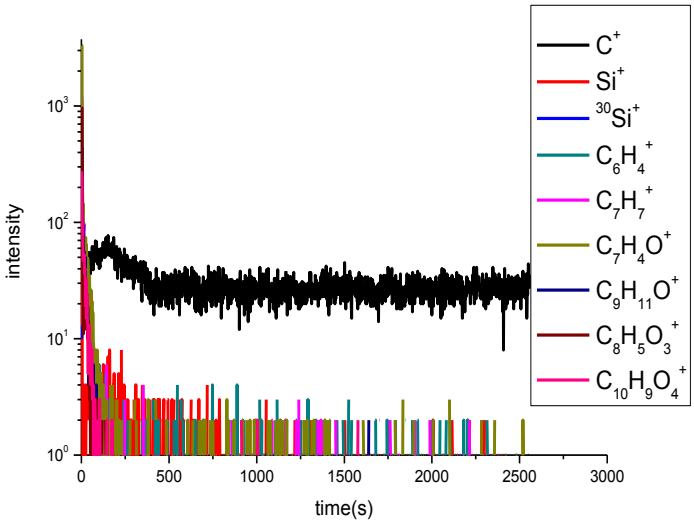

Fig. 47 - C_{60} depth profile of PC/PET blend 3:1, without NO.

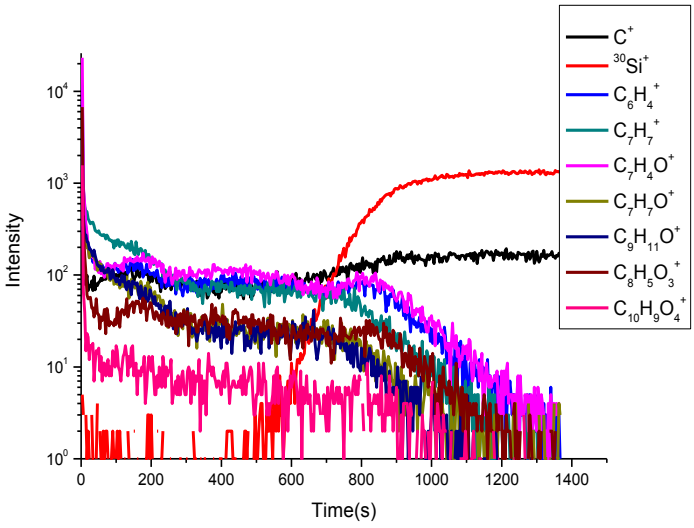

Fig. 48 - C_{60} depth profile of PC/PET blend 3:1, with NO ~10^{-5} mbar.

3.4.3 Polymer/additive systems

The polymers chosen are PMMA, PS and PETi, which characteristics have been widely discussed in the previous sections. Two commercially available antioxidant additives were used, namely Irgafos 168® (Tris (2,4-di-tert-butylphenyl)phosphite) and Irganox 1010® (Pentaerythritol Tetrakis(3-(3,5-di-tert-butyl-4-hydroxyphenyl)propionate)).

The structures of these additives are reported in figure 49.

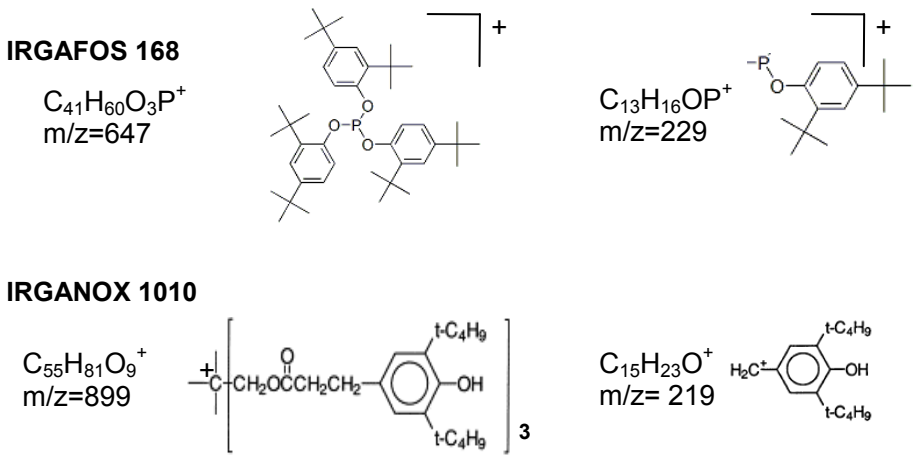

Fig. 49 Additives: structures and fragments monitored during depth profiles.

ToF-SIMS spectra of the polymer-additive thin films, reported in the figures from 50 to 55, show the presence of the additive-related fragments.

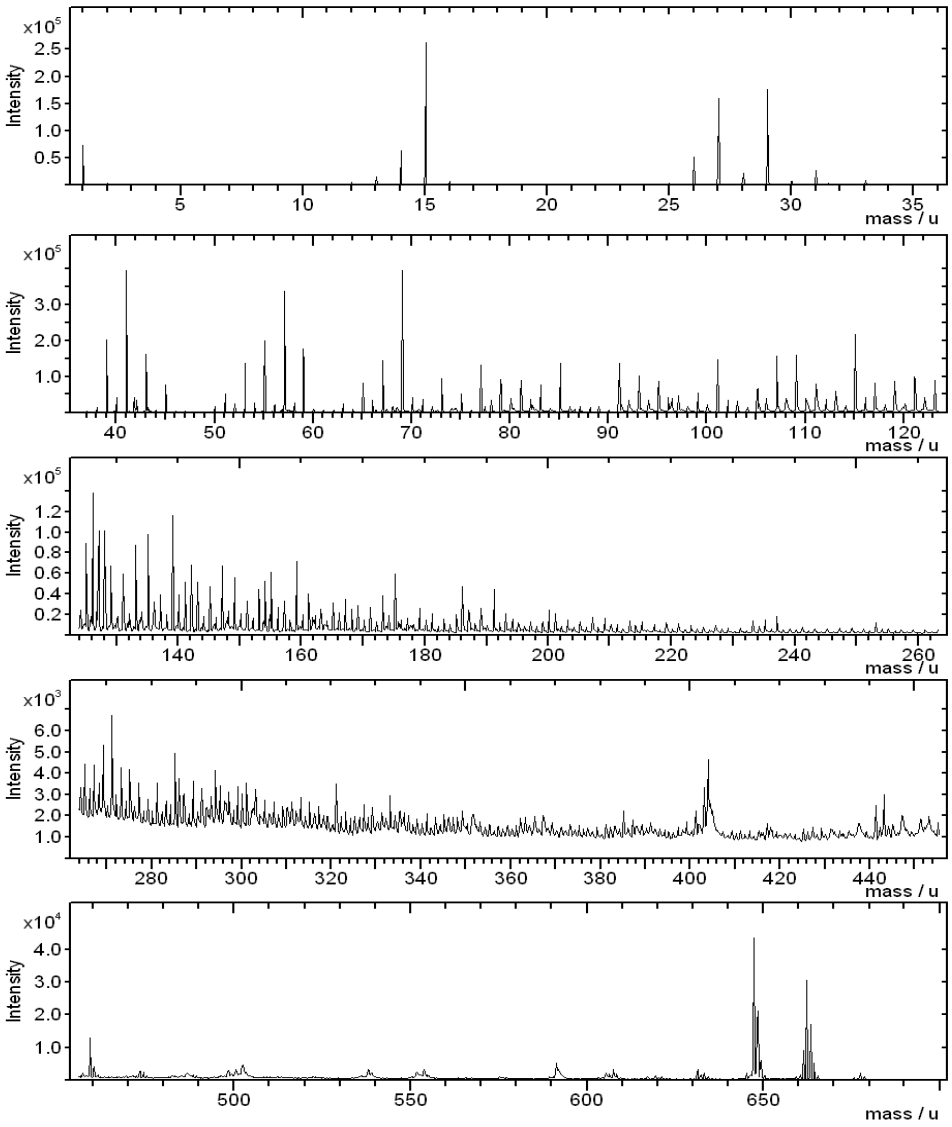

Fig. 50 – Positive-ion ToF SIMS spectrum of PMMA+irgafos

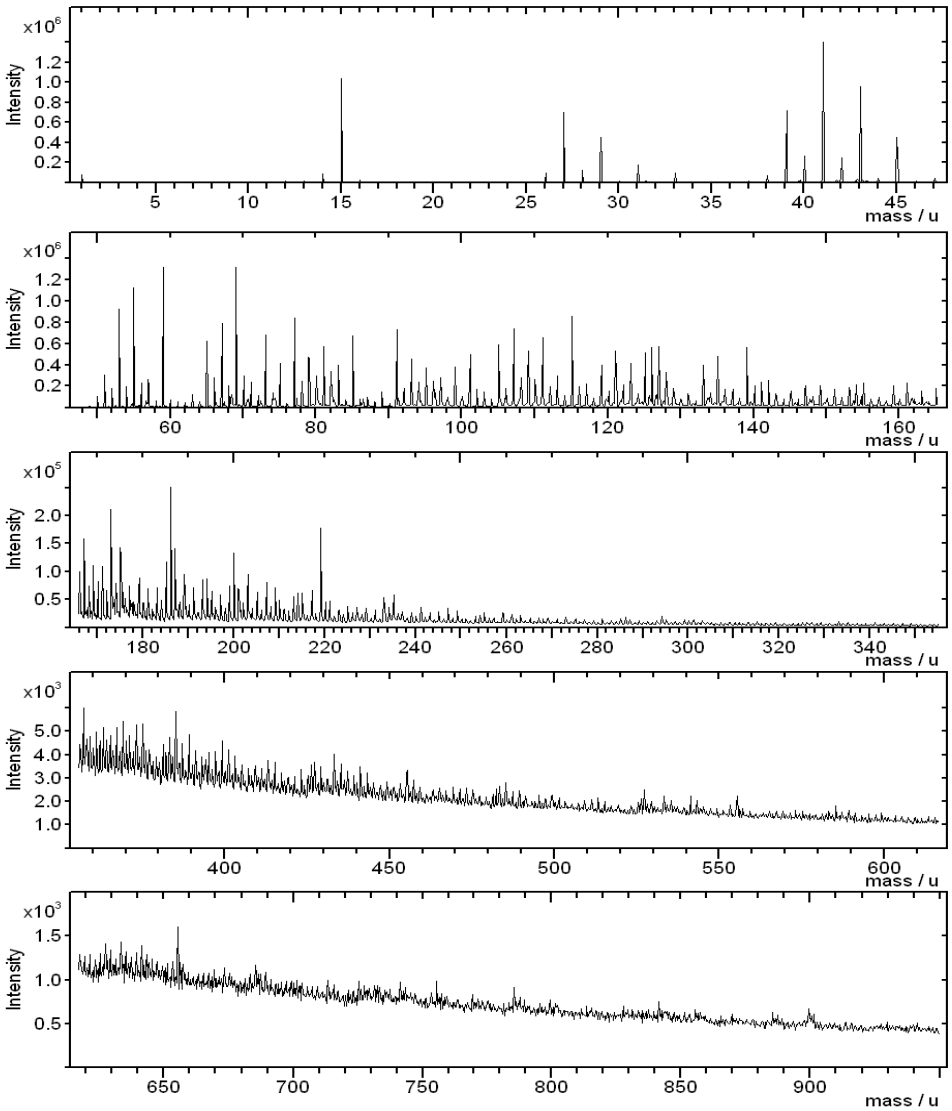

Fig. 51 - Positive-ion ToF SIMS spectrum of PMMA+irganox.

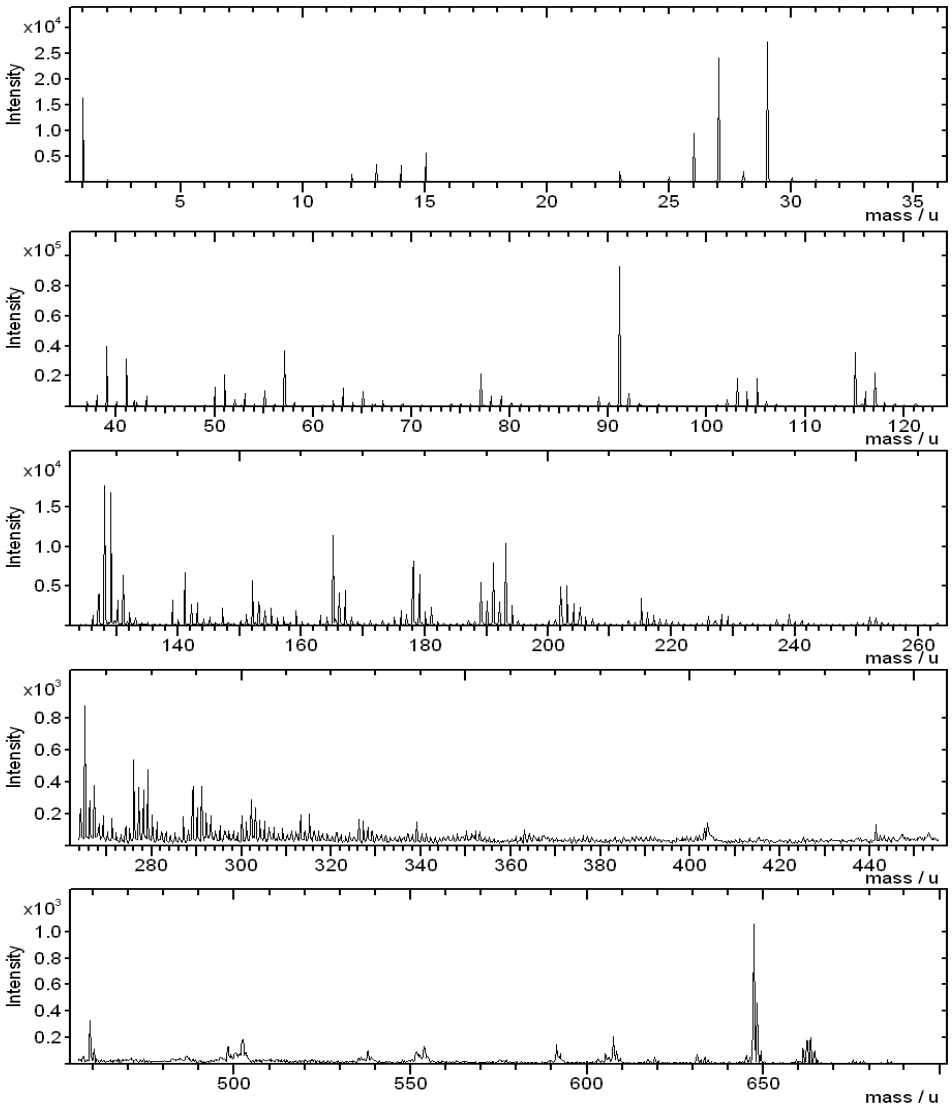

Fig. 52 – Positive-ion ToF SIMS spectrum of PS+irgafos.

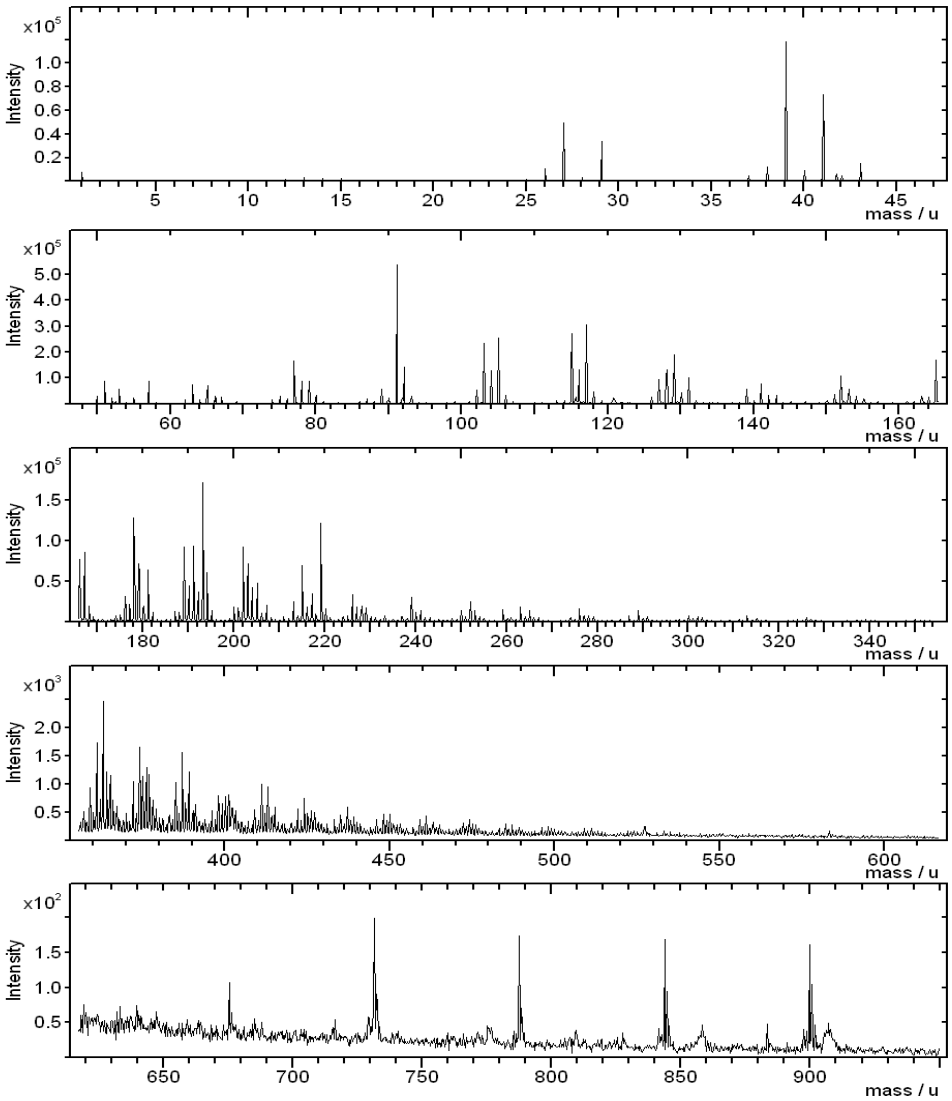

Fig. 53 - Positive-ion ToF SIMS spectrum of PS+irganox.

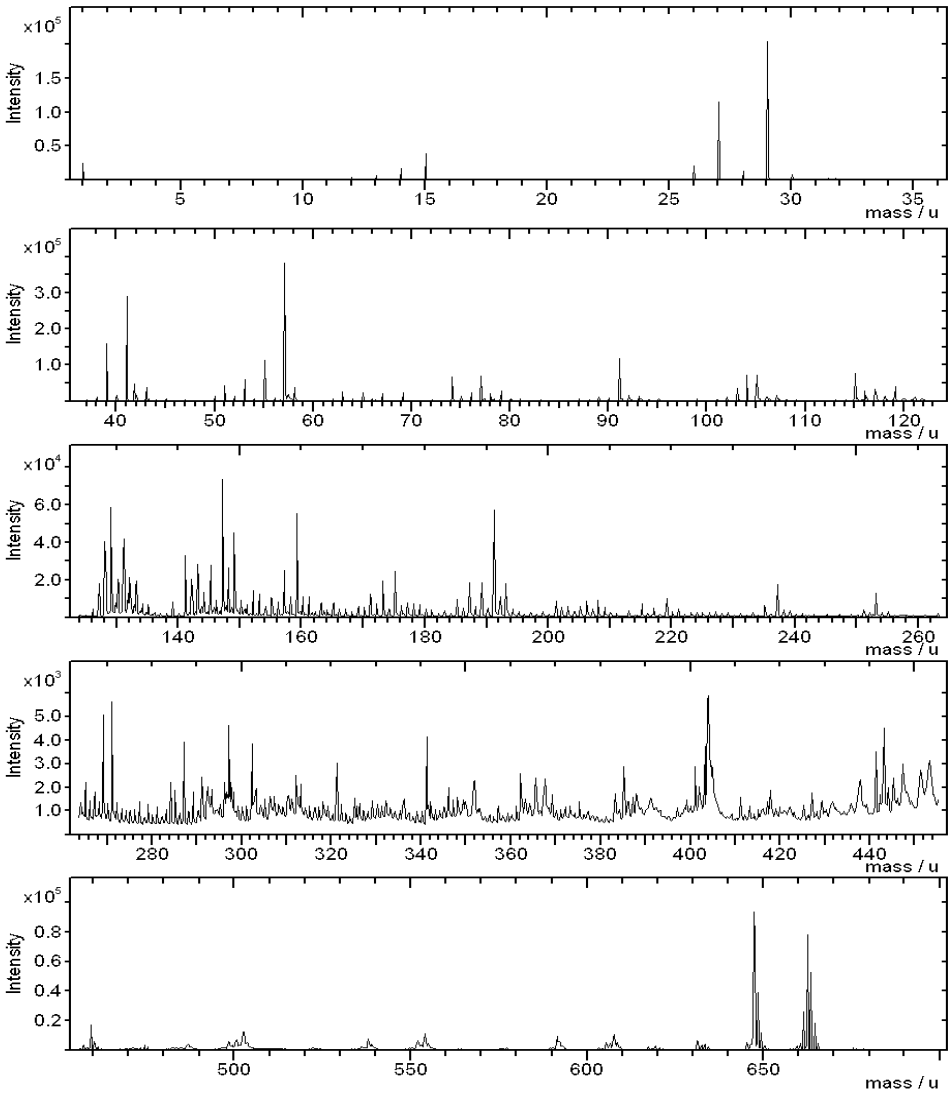

Fig. 54 – Positive-ion ToF SIMS spectrum of PETi+irgafos.

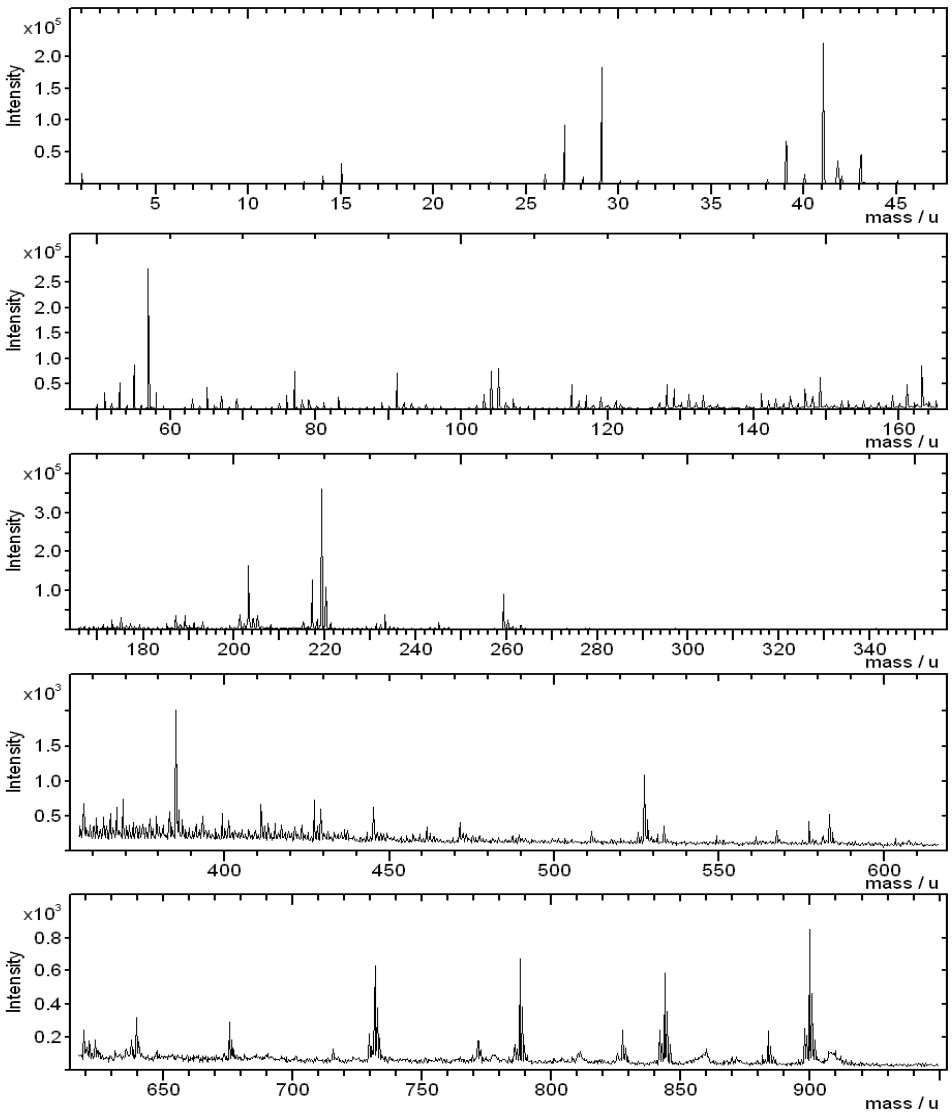

Fig. 55 – Positive-ion ToF SIMS spectrum of PETi+irganox.

In figures 56-61 the depth profiles obtained in absence of NO dosing are reported. As can be easily seen, it is confirmed that PMMA is amenable to retain molecular information along the depth. In the case of PETi, the same considerations can be done, even if with some little differences (a certain accumulation of damage is revealed by the negative slope of the molecular signals in the quasi-plateau region of the profile. In the case of PS, on the contrary, signals drops to zero beyond the static limit. The presence of additives does not affect, at least qualitatively, the appearance of the profiles. Furthermore, enhancements in sputter yields, especially in the case of PS, are observed. It must be noted that, in all the cases under investigation, the molecular ions of additives dropped to zero beyond the static limit, irrespective of the profilability or non-profilability of the host polymer.

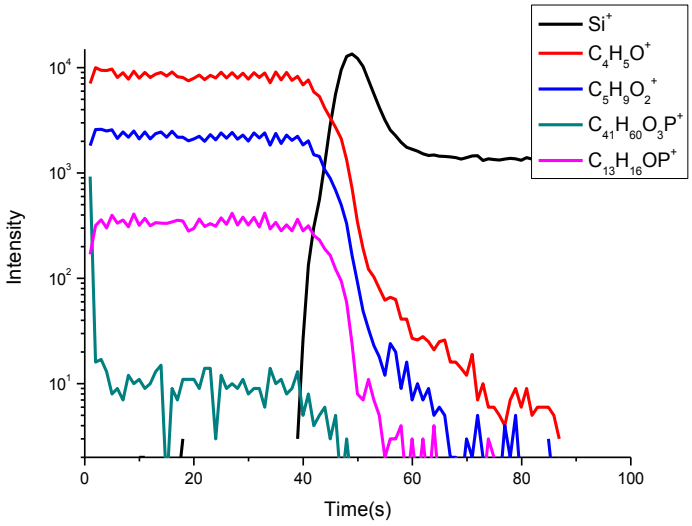

Fig. 56 - Depth profiling of PMMA + irgafos.

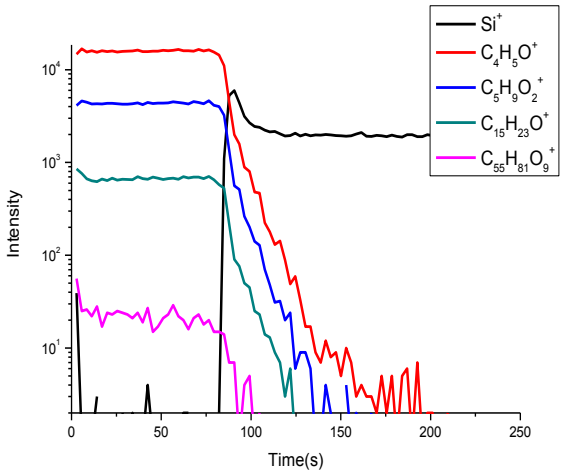

Fig.57 - Depth profiling of PMMA + irganox.

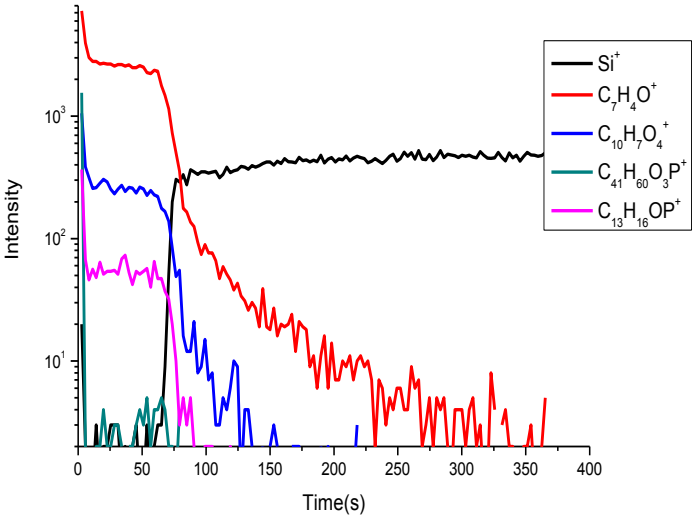

Fig.58 - Depth profiling of PETi + irgafos

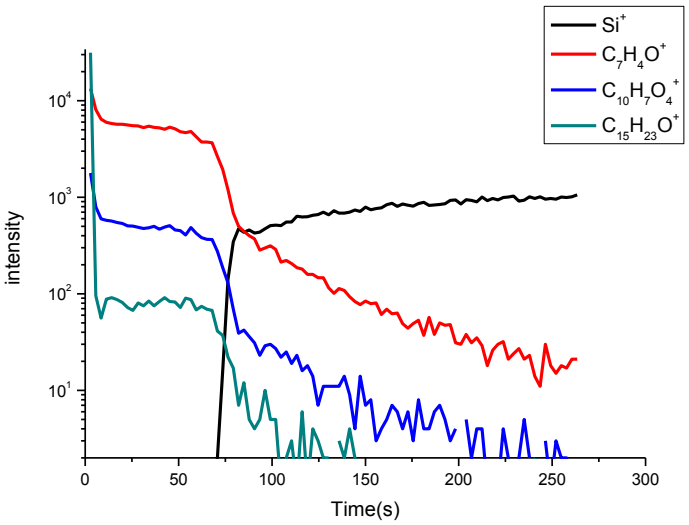

Fig. 59 - Depth profiling of PETi + irganox.

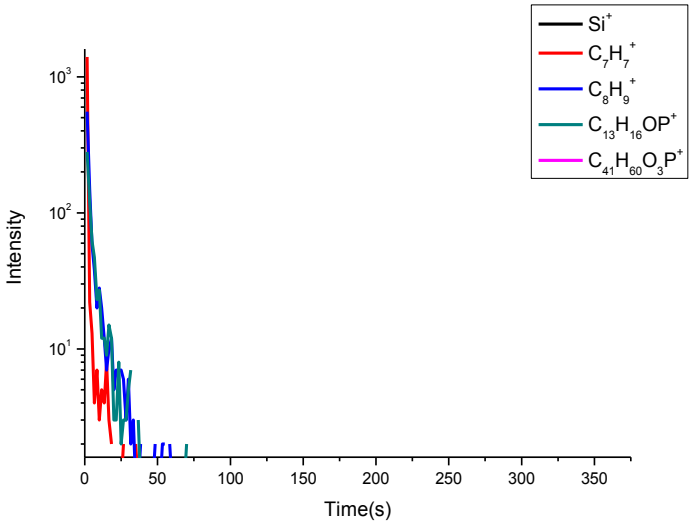

Fig. 60 - Depth profiling of PS + irgafos.

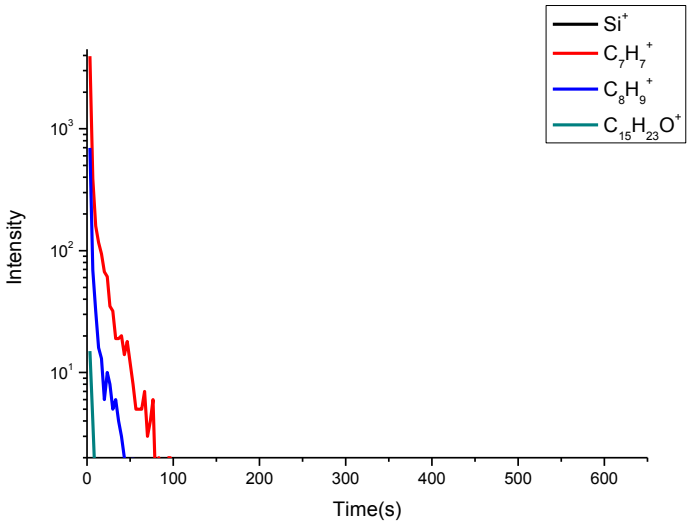

Fig.61 - Depth profiling of PS + irganox

The profiles obtained in the presence of the radical scavenger (NO) are reported in the figures 62-67.

The presence of additives does not change the overall behaviour of the matrix polymers, as they are all profilable, similarly to the corresponding pure polymers. Indeed PS becomes amenable of successful depth profile, with retention of structure-related signals and increase of the sputter yield of more than one order of magnitude, while PMMA and PETi are not affected (or slightly affected in the case of PETi) by the presence of the additive. So we can concluded that the presence of antioxidant additives does not appear to significantly interfere with the effect of nitric oxide, thus opening the perspectives of applications of this technique also to the investigation of polymer additive systems.

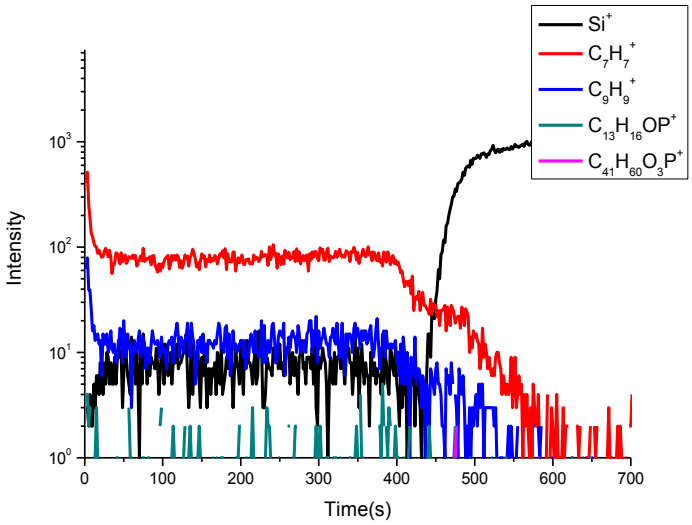

Fig. 62 - Depth profiling of PS+irgafos with NO-dosing.

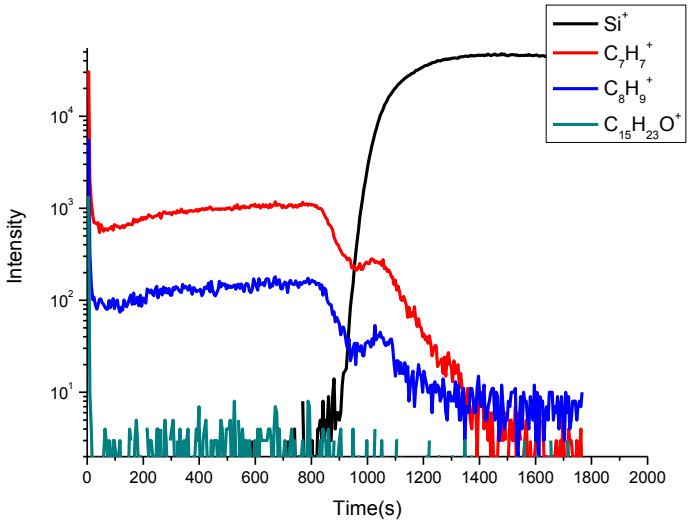

Fig. 63- Depth profiling of PS+irganox with NO-dosing.

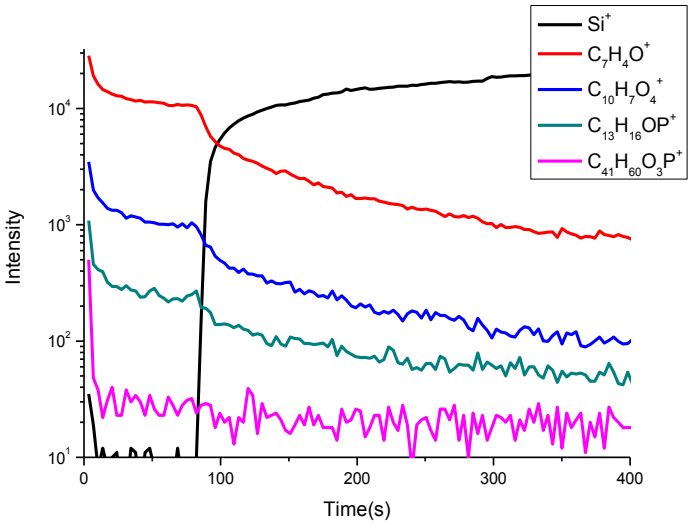

Fig. 64 - Depth profiling of PETi+irgafos with NO-dosing.

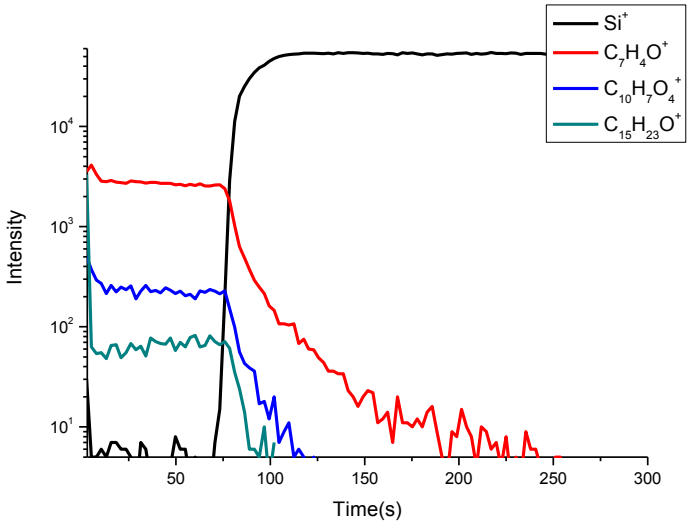

Fig. 65 - Depth profiling of PETi + irganox with NO-dosing.

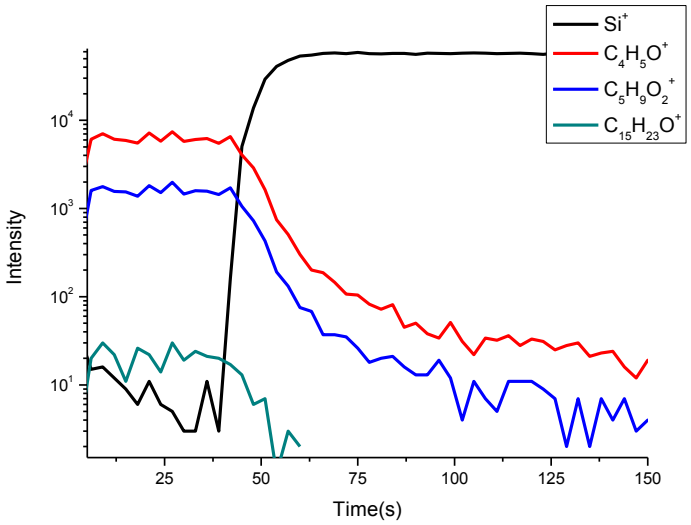

Fig. 66 - Depth profiling of PMMA +irgafos with NO-dosing.

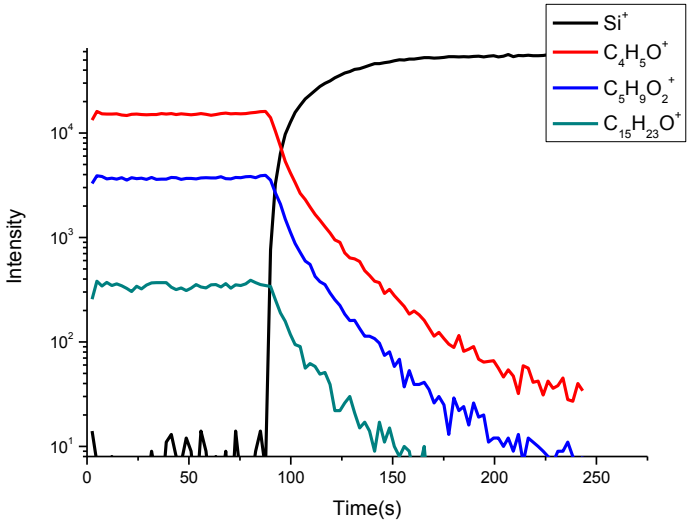

Fig. 67 - Depth profiling of PMMA + irganox with NO-dosing.

4. Conclusions

During this PhD work the effect of the introduction nitric oxide, a well known radical scavenger, in the residual atmosphere of the SIMS spectrometer (NO-dosing) during cluster beam depth profiling of polymer based films, either single- or multicomponent systems, was studied. The general idea underlying the thesis project was that of developing a method for interfering with the ion-beam initiated reaction pathways that lead to accumulation of damage in the subsurface of polymers, that in many cases prevents the possibility of following, along the sample depth, secondary ion signals that are related with the original structure of the polymer. In other words, the idea was that of extending, by exploiting chemical methods, the "molecular depth profiling" capabilities of cluster ion beams (and fullerene beams in particular, that in the recent years constituted a major breakthrough for the in-depth investigation of organic and polymer films. With our "nitric-oxide assisted C_{60}-SIMS" methodology, successful C_{60} molecular depth profiles of PS, PAMS, PC were obtained, while the same polymers cannot be profiled successfully in the standard conditions of C_{60}-SIMS, i.e. in the absence of NO, because of their tendency to accumulate damage by increasing accumulation of crosslinks (type I behaviour). Quite interestingly, the behaviour of polymers like PMMA or PAA that, in virtue of their tendency to chain scission and depolymerisation under cluster ion beam irradiation (type II behaviour), give rise to molecular depth profiling in the absence of NO, is negligibly affected by NO dosing. Depth profiling of polymers with intermediate behaviour, such as polyethyleneterephtalate-co-isophtalate, took as well advantage from the use of NO dosing.

In addition to the above single-layer pure polymers, the investigation was extended to other systems in which polymers with different behaviour (type I or

II) under fullerene beam irradiation were co-existing, as in the case of multilayered systems, including hybrid polymer/metal multilayers, immiscible polymer blends, properly chosen random copolymers and additive-containing systems. In all the examined cases the general observation is that the presence of nitric oxide during C_{60} has a positive uniforming effect, not only on the possibility of obtaining molecular in-depth information also in the presence of "difficult" polymers, but also on the erosion rates, even in the presence of inorganic interlayers. In some respects, NO dosing appears to play – in polymer depth profiling – a role similar to that played by oxygen dosing in uniforming the "matrix effect" in depth profiling of inorganic layers. This makes the nitric oxide-assisted C_{60} depth profiling a very promising tool, also in view of the fact that the novel gas cluster ion beams, that appear to be very effective in quasi-damageless polymer molecular depth profiling, experience difficulties when dealing with hybrid organic-inorganic systems due to their very low (sometimes negligible) sputtering yields on inorganics.

Moreover, the experiments performed with nitric oxide allowed to gain some insight into the chemical processes triggered by cluster beam irradiation of polymers. In particular, the experiments on the effect of the NO pressure on C_{60}-irradiated polystyrene show an increase of the intensities of polymer-related fragments, in combination with a decrease of damage-related signals and a parallel increase of sputtering rate. These findings are interpreted in terms of competition between scission and cross-linking reactions pathways, that is influenced (with disfavouring effect on cross-linking) by the radical inhibition performed by nitric oxide. Also, the above results supply a further clear demonstration of the strict relationship between the presence of an efficient mechanism of ablation (that

appears to be hindered by the cross-linking pathways) and possibility of obtaining a “molecular depth profiling, in agreement with previsions of simulations present in the literature.

In conclusion, the experimental results obtained in this Ph.D. work by using the novel “NO-assisted C_{60}-SIMS depth profiling”, candidate this technique, possibly joined with the use of focused ion beams in a dual ion beam arrangement, as a very promising tool for molecular spatially resolved investigation of complex polymer-based systems, thanks to the uniforming effect of nitric oxide on of polymers with largely different behaviours under cluster beam irradiation, in terms of both emission of useful structure-related fragments and of sputtering yield. All of this can be a certain relevance also considering the need of spatially resolved chemical characterization tools in many technological fields exploiting polymer-based micro- and nano-structured systems.

Appendix : Materials and methods

About half micrometer-thick films of polymer films have been obtained by means of spin coating deposition, in which a solution (~3%) of the polymer is spread on a plate rotating at a very high speed (thousands rpm), in order to allow the solvent to evaporate and in this way leaving a thin film of the polymer deposited on the substrate, in our case either a silicon wafer or a polymer plate. More details of the whole spin coating process are reported in the following.

Once prepared, the samples were investigated by means of ToF-SIMS, in the "static mode", to obtain highly informative surface mass spectra, and in the "dynamic mode", for gaining in-depth information. Again, more details are reported in the following.

Materials

All the materials used were commercially available:

- Polystyrene (PS) - Scientific Polymer, av. Mw 280000;
- Poly-α-methylstyrene (PAMS) – Aldrich, av. Mw 60000;
- Polymethylmethacrylate (PMMA) - Scientific Polymer, av. Mw 540000;
- Polyacrylic Acid (PAA) - Polisciences, av. Mw ~100000;
- Polyethylene terephthalate (PET) - Scientific Polymer;
- Polyethylene terephthalate-co-isophthalate (PETi) - ICI-UK;
- Bisphenol A-Polycarbonate (PC) - Scientific Polymer, av. Mw 60000;

- Styrene 8%-co-Methylmethacrylate - Polymer Source, av. Mw 132700;
- Styrene 51%-co-Methylmethacrylate - Polymer Source, av. Mw 134300;
- Styrene 91%-co-Methylmethacrylate - Polymer Source, av. Mw 102800;
- Irgafos 168® (CIBA);
- Irganox 1010® (CIBA);

Film preparation

Homogeneous, single-layer polymer films were obtained by spin casting of polymer solutions on the substrate of choice, usually a silicon wafer or, in some instances, a PET plate. By proper choice of solvent, polymer concentration and spinning parameters (mainly rotation speed) it is possible to control the film thickness.

Briefly, a spin casting deposition is described as follows: a small amount of polymer solution is cast onto the substrate, the rotation of which then accelerates, according to the chosen spin ramp. As well as the maximum of speed is reached, this remains constant for a certain time, in order to allow the quick evaporation of the solvent, due to the generated centrifugal force, that have to be balanced with the viscosity (rapidly changing during the evaporation process). Summarizing, the film thickness depends on the solvent, on the concentration of the polymer solution, and on the rotation speed of the substrate.

Layered structures constituted by films of different polymers have been obtained in a similar way, by sequential spin casting of each polymer, and with a proper choice of the solvents, in order to avoid - during the deposition of a certain layer - the dissolution of the underlying film.

Hybrid polymer/metal layered structures have been obtained by alternating the deposition of polymer layers (following the same method above outlined) with the deposition, in a DC parallel plate sputter reactor, of ~50 nm-thick gold films[*].

Blends of polystyrene (PS)/polymethylmethacrylate (PMMA) (nominal composition 4:1 w/w), and polyethylene terephthalate (PET)/bisphenol A-polycarbonate (PC) (nominal composition 25:75 w/w) have been prepared by spin casting, by using, respectively, a 2% (w/w) solution of PS + PMMA (overall) in chloroform and a 2% (w/w) solution of PET + PC (overall) in a chloroform/hexafluoroisopropanol (9:1) mixture.

Mixed additive/polymer thin films were prepared starting from 3% overall solutions. In all the polymer/additive solutions the additive concentration was chosen to be 1% w/w with respect to the polymer.

Film thickness was generally controlled by spin casting parameters and estimated, when possible, by measuring the depth of a scratch by AFM.

The following table reports the deposition all the experimental conditions for the film preparation, and the estimated thicknesses of the samples prepared. In the adopted notation, the sequence of layers is given from the uppermost layer (left) to the substrate (right).

[*] Acknowledgments for sputter deposition: Prof.ssa G. Malandrino and co-workers

Table 1 Conditions adopted for film preparation.					
Film structure	Material	Solvent	Conc. (w/w)	rpm	thickness
PS/Si	PS	chloroform	3%	2500	0,5÷1μm
PMMA/Si	PMMA	chloroform	3%	2500	~0.5μm
PETi/Si	PETi	chloroform	3%	2500	0,5÷1μm
PC/Si	PC	chloroform	3%	2500	0,5÷1μm
PAA/Si	PAA	water/methanol	3%	1500	~0.5μm
PAMS/Si	PAMS	chloroform	3%	2500	0,5÷1μm
PBzMA/Si	PBzMA	chloroform	3%	2500	0,5÷1μm
PS/PMMA/Si	PMMA	acetone	3%	1500	~0.5μm
	PS	1-chloropentane	3%	1500	~0.5μm
PS/PMMA/PAA/PETi/Si	PETi	chloroform	3%	1500	~0.5μm
	PAA	water/methanol	3%	1500	~0.5μm
	PMMA	acetone	3%	1500	~0.5μm
	PS	1-chloropentane	3%	1500	~0.5μm
PS/Au/PMMA(Co)/Au/PETi/Si (*) (**)	PETi	chloroform	3%	1500	~0.5μm
	PMMA	acetone*	5%	2000	~0.5μm
	PS	1-chloropentane	5%	2000	~0.5μm
PS/Au/PMMA(Co)/PET (*) (**)	PMMA	acetone*	5%	2000	0,5÷1μm
	PS	1-chloropentane	5%	2000	0,5÷1μm
S8%-co-MMA92%/Si	S8%-co-MMA92%	chloroform	3%	2500	0.5μm
S51%-co-MMA49%/Si	S51%-co-MMA49%	chloroform	3%	2500	0.5μm
S91%-co-MMA9%/Si	S91%-co-MMA9%	chloroform	3%	2500	0.6μm
PS-PMMA 4:1 blend/Si	PS	chloroform	2% overall	500	0,5÷1μm
	PMMA	chloroform			

PET-PC 25:75 blend/Si	PET	9:1 chloroform/ hexafluoro-isopropanol	2% overall	500	0,5÷1μm
	PC	chloroform			
PS+irgafos 168/Si (***)	PS	chloroform	3% overall	3000	~0,7 μm
	Irgafos 168®				
PS+irganox 1010/Si (***)	PS	chloroform	3% overall	3000	~0,6 μm
	Irganox 1010®				
PMMA+irgafos 168/Si (***)	PMMA	THF	3% overall	3000	~0,4 μm
	Irgafos 168®				
PMMA+irganox 1010/Si (***)	PMMA	chloroform	3% overall	3000	~0,8 μm
	Irganox 1010®				
PETi+irgafos 168/Si (***)	PETi	chloroform	3% overall	3000	~0,4 μm
	Irgafos 168®				
PETi+irganox 1010/Si (***)	PETi	chloroform	3% overall	3000	~0,4 μm
	Irganox 1010®				

Notes:

*) $Co(CH_3COO)_2$ in ethanol (saturated solution), diluted 1:100 in acetone.

**) deposition of gold layers (~50 nm thick): 2 cycles (3 min.), 20 mA, $P_{Ar} = 2x10^{-1}$ mbar

***) additives concentration 1% with respect to the polymer

ToF-SIMS measurements

Samples were investigated by means of a ToF-SIMS apparatus (TOFSIMS IV, ION-TOF GmbH), in the "static SIMS mode", in order to obtain mass spectra and chemical maps, and in the "dynamic mode", in order to obtain in-depth information. In static SIMS mode, a focused pulsed primary ion beam (Bi^+ or Bi_3^+, 25 keV, ~0.1 pA, pulse width <1 ns) was rastered over an area of 200 x 200 μm^2 (see Appendix B for further information about the technique). The measurement time was established in order to keep the fluence below the value of $2x10^{11}$ ions cm^{-2}, in order to accomplish with the "static limit". Depth profiles (dynamic SIMS mode) were obtained in dual beam mode[76], i.e. by alternating a sputtering cycle using a fullerene beam (C_{60}^{++}, 20 keV, ~1 nA) and a measuring cycle with a bismuth beam (Bi_3^+, 25 keV, ~0,1 pA, as in the case of the static mode). In order to avoid artefacts due to the sputter crater edge, the analysis area (130 x 130 μm^2) was set smaller and concentric to the sputtered area (200 x 200 μm^2). Due to the characteristics of the time-of-flight measurements, a complete spectrum is acquired per each individual voxel (i.e. a tri-dimensional small volume), thus allowing the parallel acquisition of all masses (in the chosen mass range, typically 1-3500 u) along the depth profile. All the acquired data are stored in a raw data that contain a 3D information from which it is possible to reconstruct spectra from a certain sample region, 2D or 3D images, depth profiles. In the following, the depth profiles displayed have been obtained by monitoring a few masses that are related with the structure of each polymer present. A summary of the characteristic fragments is reported in table 2.

Table 2 List of the monitored signals for each polymer.

MATERIAL	MONITORED SIGNALS
Polystyrene (PS)	$C_7H_7^+$, m/z = 91 $C_8H_7^+$, m/z = 103 $C_9H_7^+$, m/z = 115
Polymethylmethacrylate (PMMA)	$C_2H_3O_2^+$ m/z = 59 $C_4H_5O^+$, m/z = 69 $C_5H_9O_2^+$, m/z = 101
Polyacrylic acid (PAA)	$C_3H_5^+$, m/z = 41 $C_3H_3O^+$, m/z = 55 $C_3H_5O_2^+$, m/z = 73 $C_7H_7^+$, m/z = 91
Poly-α-methylstyrene (PAMS)	$C_7H_7^+$, m/z = 91 $C_7H_9^+$, m/z = 105
Polyethylene terephthalate(PET) Polyethylene terephthalate-co-isophthalate (PETi)	$C_6H_4^+$, m/z = 76 $C_7H_4O^+$, m/z = 104 $C_8H_5O_3^+$, m/z = 149
Bisphenol A-Polycarbonate (PC)	$C_7H_7O^+$, m/z = 107 $C_9H_{11}O^+$, m/z = 135
Styrene-Methylmethacrylate (S-MMA) random copolymers	$C_7H_7^+$, m/z = 91 $C_8H_7^+$, m/z = 103 $C_9H_7^+$, m/z = 115 $C_2H_3O_2^+$, m/z = 59 $C_4H_5O^+$, m/z = 69 $C_5H_9O_2^+$, m/z = 101
Irgafos 168®	$C_{13}H_{16}OP^+$, m/z = 229 $C_{41}H_{60}O_3P^+$, m/z = 647
Irganox 1010®	$C_{15}H_{23}O^+$, m/z = 219 $C_{55}H_{81}O_9^+$, m/z = 899

For each sample measurements have been performed in the "standard" way (i.e. in UHV, residual gas pressure ~ $1x10^{-8}$ mbar) or in the presence of nitric oxide.

Nitric oxide dosing was obtained by introducing in the UHV chamber, in the proximity of the sample surface, a partial pressure of NO (typically 1.5×10^{-5} mbar) by means of a precision leak valve with an automatic regulation of the flux in order to maintain the chosen pressure.

References

[1] A. Benninghoven, *Angew. Chem* ., 106 (**1994**) 1075 –1096, *Angew. Chem*. Int. Ed. Engl .**1994**, 33, 1023 –1043

[2] A. Benninghoven; H. W. Werner; F.G. Rudenauer, *Secondary Ion Mass Spectrometry: Basic Concepts, Instrumental Aspects, Applications and Trends*, Wiley-Interscience**,** Chichester, **1987**

[3] S. Pignataro, A. Licciardello, *Gazzetta Chimica Italiana*, vol. 120, **1990**, p. 351-363

[4] S. Pignataro, G. Marletta, *Metallized Plastics* ,2 (**1992**) 269-81

[5] C.M. Mahoney, *Mass Spectrom. Rev*., 29 (**2010**) 247

[6] F. Kollmer*, Applied Surface Science* , 231 –232 (**2004**) 153 –158

[7] K. Ichiki, S. Ninomiya, Y. Nakata, Y. Honda, T. Seki, T. Aoki, J. Matsuo, *Appl. Surf. Sci.* 255 (**2008**) 1148 –1150

[8] R. Moellers, R. Kersting, F. Kollmer, D. Rading, T. Grehl, E. Niehuis, in *Proceedings SIMS Europe 2004*, Muenster, **2004**, p.106

[9] R. Moellers, N. Tuccitto, V. Torrisi, E. Niehuis, A. Licciardello, *Appl. Surf. Sci.*, 252 (**2006**) 6509 –6512

[10] C. Szakal, S. Sun, A. Wucher, N. Winograd., *Appl. Surf. Sci.* 231 –232 (**2004**) 183 – 185

[11] D. Weibel, S. Wong, N. Lockyer, P. Blenkinsopp, R. Hill, J. C. Vickerman*, Anal Chem* ,75 (**2003**) 1754 –1764

[12] A. Delcorte, *Physical Chemistry Chemical Physics* ,7 (**2005**) 3395-3406

[13] R. Paruch, L. Rzeznik, M. F. Russo, B. J. Garrison and Z. Postawa*, J.Phys.Chem.C* ,114 (**2010**) 5532 –5539

[14] Z. Postawa, B. Czerwinski, M. Szewczyk, E. J. Smiley, N. Winograd and B. J. Garrison, *Anal. Chem*., 75, 4402-4407 (**2003**)

[15] Z. Postawa, B. Czerwinski, M. Szewczyk, E. J. Smiley, N. Winograd and B. J. Garrison , *J. Phys. Chem. B*, 108, 7831-7838 (**2004**)

[16] M. S. Wagner, *Surf. Interface Anal.* .37 (**2005**) 42 –52

[17] M. S. Wagner*, Surf. Interface Anal.* .37 (**2005**) 53 –61

[18] M. S. Wagner, *Surf. Interface Anal.* .37 (**2005**) 62 –70

[19] G. Gillen, S. Roberson, *Rapid Commun. Mass Spectrom.*, **1998**, 12:1303–1312

[20] F. M. Green, A. G. Shard, I. S. Gilmore, M. P. Seah, *Anal. Chem*. **2009** Jan 1; 81(1):75-9

[21] J. Cheng, N. Winograd, *Anal. Chem*. 77 (**2005**) 3651–3659

[22] A. Wucher, J. Cheng, N. Winograd, *Applied Surface Science*, 255, 4 (**2008**), p. 959

[23] C.M. Mahoney, A.J. Fahey, G. Gillen, C. Xu and J. D. Batteas, *Appl. Surf. Sci.,* (**2006**) 252, 19, 6502-6505

[24] J. Cheng, A. Wucher, N. Winograd, *J. Phys. Chem. B* 110: **2006** 8329–8336

[25] A. Wucher, *Surf. Interface Anal.* **2008** 40:1545–1551

[26] A. Wucher, J. Cheng, N. Winograd *J. Phys. Chem. C* 112 **2008** (42):16550–16555

[27] A. Chapiro, *Radiation chemistry of polymeric systems*. New York & London, John Wiley & Sons. p. 712. **1962**

[28] L. Calcagno, *Nucl. Instr. Meth. Phys. Res. B* **1995**, 105: 63-70

[29] M.E. Fragalà, G. Compagnini, L. Torrisi, O. Puglisi, *Nuclear Instruments and Methods in Physics Research B*, **1998**, *141*, 169-173

[30]B. Pignataro, M.E. Fragalà, O Puglisi. *Nucl. Instr. Meth. Phys. Res. B*, **1997**, 131: 141-148

[31] A. Licciardello, M.E. Fragalà, G. Foti, G. Compagnini, O. Puglisi, *Nucl. Instr. Meth. Phys. Res. B,* **1996***, 116, 1-4,* 168-172

[32] J. Lindhard, M. Scharff, H.E. Schiøtt. Range Concepts and Heavy Ion Ranges. *Matematisk-fysiske Meddelelser Det Kongelige Danske Videnskabernes Selskab*, Vol. 33, No. 14, 1963, pp. 1-42

[33] D.Briggs and M.P.Seah, *Practical surface analysis*, Ch. 3, Wiley **1992**

[34] P. Sigmund, C. Claussen *J. Appl. Phys.* (**1981**) 52:990

[35] B. J. Garrison, Z. Postawa, *Mass Spectrom. Rev.* **2008** 27:289–315

[36] H. M. Urbassek, C. Anders, L. Sandovalan A.K. Upadhyay, *proc. of SPIE* vol.7005, 700507, **2008** , DOI:10.1117/12.784270

[37] C. Anders, H. Kirihata, Y. Yamaguchi, H. M. Urbassek*, Nuclear Instruments and Methods in Physics Research B* 255 (**2007**) 247–252

[38] M. Prasad, P. F. Conforti, and B. J. Garrison, *J. Appl. Phys*. 101, 103113 (**2007**); doi: 10.1063/1.2740340

[39] A. Delcorte, O. A. Restrepo, B. Czerwinski and B. J. Garrison, *Surface and Interface Analysis*, 45 (1), **2013**, DOI: 10.1002/sia.4926

[40] D. Rading, R. Moellers, H.-G. Cramer, E. Niehuis, *Surface and Interface Analysis*, 45 (1), **2013**, DOI: 10.1002/sia.5122

[41] Z. Postawa, L. Rzeznik, R. Paruch, M.F. Russo, N. Winograd, B. J. Garrison, *Surf.Interface Anal.* **2011**, 43, 12–15

[42] S. Ninomiya, K. Ichiki, H. Yamada, Y. Nakata, T. Seki, T. Aoki, J. Matsuo, *Rapid Commun. Mass Spectrom*., **2009**, 23:1601

[43] A. Licciardello, O. Puglisi, L. Calcagno, G. Foti, *Nuclear Instruments and Methods in Physics Research* B46 (**1990**) 338-341

[44] L. Calcagno, G. Campagnini, G. Foti, *Nucl. Instr. and Meth. B* 65 (**1992**) 413

[45] L. Calcagno, G. Foti, *Nucl. Instr. and Meth. B* 59/60 (**1991**) 1153

[46] L. Calgagno, R. Percolla and G. Foti, *Nucl. Instr. and Meth. B* 95 (**1995**) 59

[47] S. Klaumünzer , Q.Q. Zhu, W. Schnabel, G. Schumacher, *Nuclear Instruments and Methods in Physics Research B* 116 (**1996**) 154-158

[48] P. E. Kennedy, B. J. Garrison, *Surface and Interface Analysis*, 45 (1), **2013**, DOI: 10.1002/sia.5022

[49] D. A. Brenes, Z. Postawa, A. Wucher, P. Blenkinsopp, B. J. Garrison, N. Winograd, *Surface and Interface Analysis*, 45 (1), **2013**, DOI: 10.1002/sia.5077

[50] N. Mine, B. Douhard , L. Houssiau, *Applied Surface Science*, **2008**, 255:973–976

[51] L. Houssiau , N. Mine , *Surf. Interface Anal*., **2010**, 42:1402-1408

[52] T. Mouhib, A. Delcorte, C. Poleunis, P. Bertrand, *J. Am. Soc. Mass Spectrom*. **2010**, 21, 2005

[53] T. Mouhib, A. Delcorte, C. Poleunis, P. Bertrand, *Surface and Interface Analysis*, 45 (1), **2013**, DOI: 10.1002/sia5043

[54] A. Licciardello, presented at SIMS XVII, International Conference on Secondary Ion Mass Spectrometry, Toronto (Canada) Sep **2009**

[55] D. Sapuppo, G. Zappalà, V. Spampinato, N. Tuccitto, A. Licciardello, presented at SIMS Europe 2010, Muenster (Germany), Sep **2010**

[56] D. Sapuppo, G.Zappalà, V.Spampinato, N. Tuccitto, A. Torrisi, A. Raudino, A. Licciardello, presented at SIMS XVIII, International Conference on Secondary Ion Mass Spectrometry, Riva del Garda (Trento, Italy) Sep **2011**

[57] D. Sapuppo, G. Zappalà, V. Cristaudo, A. Licciardello, presented at SIMS Europe 2012, Muenster (Germany), Sep **2012**

[58] O. Puglisi, A. Licciardello, S. Pignataro, L. Calcagno, G. Foti, *Radiat. Eff.* (**1986**) 98:161–170

[59] O. Puglisi, A. Licciardello, L. Calcagno, G. Foti, *Nucl. Instr Meth. Phys. Res. B* (**1987**) 19/20:865–871

[60] O. Puglisi, A. Licciardello, L. Calcagno, G. Foti, *J. Mater. Res.* (**1988**) 3(6):1247–1252

[61] R. Wilken, A. Holländer, J. Behnisch, *Macromolecules* (**1998**), 31, 7613-7617

[62] R. Wilken, A. Holländer, J. Behnisch, *Surface and Coatings Technology* 116–119 (**1999**) 991–995

[63] C. M. Mahoney, A. J. Fahey, G. Gillen, C. Xu, J. D. Batteas., *Anal. Chem.* (**2007**), 79, 837

[64] T. Venkatesan , L. Calcagno, B. S. Elman, G. Foti, Ion beam effects in organic molecular solids and polymers. In: *Ion Beam Modification of Insulators*, P.Mazzoldi and G.W.Arnold (eds.) Elsevier, Amsterdam, (**1987**), p.301-379

[65] J. Cheng, A. Wucher, N. Winograd, *J. Phys. Chem. B* (**2006**) 110, 8329-8336

[66] M. S. Wagner, *Anal. Chem*., (**2005**), 77:911–922

[67] J. Cheng, N. Winograd., *Applied Surface Science*, (**2006**), 252:6498–6501

[68] L. Zheng, A. Wucher, N. Winograd, *J. Am. Soc. Mass Spec*., (**2008**), 19:96–102

[69] D. Mao, A. Wucher, D. A. Brenes, C. Lu, N. Winograd, *Analytical Chemistry,* (**2012**), 84:3981-89

[70] E. Niehuis, R. Moellers, D. Rading, H. G. Cramer, R. Kersting, *Surface and Interface Analysis*, 45 (1), **2013**, DOI: 10.1002/sia.5079

[71] N. Wehbe, T. Tabarrant, J. Brison, T. Mouhib, A. Delcorte, P. Bertrand, R. Moellers, E. Niehuis, L. Houssiau, *Surface and Interface Analysis*, 45 (1), **2013**, DOI: 10.1002/sia.5121

[72] A. Auditore, F. Samperi, C. Puglisi, A. Licciardello, *Composites Science and Technology* 63 (**2003**) 1213–1219

[73] A. Licciardello, A. Auditore, F. Samperi, C. Puglisi, *Applied Surface Science* 203-204 (**2003**) 556-560

[74] L. Houssiau, N. Mine, *Surf. Interface Anal.* (**2011**) 43, 146

[75] S. Iida, T. Miyayama, N. Sanada, M. Suzuki, G. L. Fisher, S. R. Bryan, *Surf. Interface Anal.* (**2011**) 43, 214

[76] Iltgen, K., C. Bendel, E. Niehuis, A. Benninghoven: *TOF-SIMS Depth-Profiling with a Dual-Beam Technique*, in : Secondary Ion Mass Spectrometry (SIMS X), A. Benninghoven, B. Hagenhoff, H. W. Werner (Eds), Wiley & Sons, p. 375, **1997**